

# 3 kW dual-phase LLC demo board

Using 600 V CoolMOS™ CFD7 and digital control by XMC4400

## About this document

### Scope and purpose

This document describes the design and performance of a 3 kW dual-phase LLC demo board (EVAL\_3kW\_2LLC\_CFD7) intended for use in the isolated HV DC-DC stage of an SMPS for telecom and industrial applications.

This is a high-performance example with a complete Infineon solution, including HV and LV power MOSFETs, controllers and drivers, demonstrating a very effective way to design the HV DC-DC stage of a telecom rectifier or industrial SMPS that meets the highest standards of efficiency and reliability. The additional benefit of a very flat efficiency plot is also achieved through a mix of proper control techniques and best-in-class power device selection.

Key Infineon products used to achieve this performance level include:

- 600 V CoolMOS™ CFD7 SJ MOSFET [IPW60R031CFD7](#)
- Isolated gate drive [1EDI60N12AF](#)
- SR MOSFETs OptiMOS™ [BSC093N15NS5](#)
- Advanced dual-channel gate drive [2EDN7524](#)
- [XMC4400](#) microcontroller
- Bias QR Flyback controller [ICE2QR2280Z](#)

As well as design information and documentation for the LLC converter, the reader will receive additional information on how the 600 V CoolMOS™ CFD7 behaves in LLC applications and the associated benefits, how the high-performance magnetics design can be approached, and insights into how to develop dual-phase LLC converters in similar power ranges adapted to specific requirements.

### Intended audience

This document is intended for design engineers who wish to evaluate high-performance topologies for High-Power (HP) SMPS converters, and develop an understanding of the design process and how to apply the multi-phase LLC design methods to their own system applications.

*Note: General knowledge about the resonant half-bridge (HB) LLC converter principle of operation is required for proper comprehension of the concepts reported in this paper.*

### Keypoints

- Demonstrates dual-phase LLC design achieving flat efficiency from light to full load using phase shedding and current balancing
- Provides insights into GUI-based configuration for loop compensation, SR management, and dynamic control tunings
- Highlights benefits of using CoolMOS™ CFD7 and OptiMOS™ 5 in achieving high efficiency and reliability in telecom and industrial SMPS designs
- Explains digital control implementation with XMC4400 for adaptive dead time, capacitive mode prevention, and fault protection

## 3 kW dual-phase LLC demo board

### Using 600 V CoolMOS™ CDF7 and digital control by XMC4400

---

#### About this product family

- Describes practical methods to overcome current imbalance in parallel resonant converters without added conversion stages

#### About this product family

##### Product family

Infineon's 3 kW dual-phase LLC demo board leverages [600 V CoolMOS™ CDF7](#) SJ MOSFETs and XMC4400 digital control to deliver exceptional efficiency and reliability. Designed for telecom and industrial SMPS, it features phase shedding, advanced protection, and a flat efficiency curve – ideal for high-density, high-performance power conversion.

##### Target applications

- [Consumer electronics](#)
- [Industrial applications](#)
- [Home appliances](#)
- [Server](#)
- [Telecom](#)
- [Renewables](#)

# 3 kW dual-phase LLC demo board

Using 600 V CoolMOS™ CDF7 and digital control by XMC4400

## Table of contents

### Table of contents

<b>About this document.....</b>	<b>1</b>
<b>About this product family .....</b>	<b>2</b>
<b>Table of contents .....</b>	<b>3</b>
<b>1 Introduction.....</b>	<b>5</b>
<b>2 Dual-phase HB LLC design concept .....</b>	<b>6</b>
2.1 Current sharing and phase shedding .....	6
2.1.1 The design challenges.....	6
2.1.2 Proposed implementation.....	10
2.2 Reliability features .....	13
2.3 Graphical User Interface (GUI) .....	16
<b>3 Board description .....</b>	<b>18</b>
3.1 Main requirements in the technical specification.....	18
3.2 General overview of the final design .....	18
3.3 Infineon components.....	19
3.3.1 Primary HV MOSFETs 600 V CoolMOS™ CFD7.....	19
3.3.2 Isolated gate drive 1EDI60N12AF.....	20
3.3.3 SR MOSFETs OptiMOS™ BSC093N15NS5.....	20
3.3.4 Advanced dual-channel gate drive 2EDN7524 .....	21
3.3.5 XMC4400 microcontroller .....	21
3.3.6 Bias QR Flyback controller ICE2QR2280Z.....	22
3.4 Board schematics.....	23
3.4.1 LLC switching power stage .....	23
3.4.2 Synchronous rectification and secondary stage.....	24
3.4.3 Control board .....	25
3.4.4 Bias board (auxiliary converter) .....	26
3.5 Magnetic components.....	27
3.5.1 HB LLC main transformer .....	27
3.5.2 LLC resonant choke.....	28
3.5.3 Auxiliary transformer .....	29
<b>4 Digital control features .....</b>	<b>30</b>
4.1 Resources and implementation concept .....	30
4.1.1 Resources (peripherals) .....	30
4.1.2 Implementation concept.....	31
4.2 Current sharing and phase shedding .....	33
4.3 Hard-commutation prevention and capacitive mode detection .....	36
4.3.1 Hard-commutation prevention .....	36
4.3.2 Capacitive mode detection and prevention .....	38
4.4 Protections .....	38
4.4.1 Overcurrent protection.....	39
4.4.2 Input and output voltage monitoring .....	40
4.4.3 Other protections.....	40
4.5 Burst mode and SR management.....	41
4.6 Adaptive dead time .....	43
4.7 Loop compensation parameters .....	43
4.8 Graphical User Interface (GUI) .....	44
<b>5 Performance evaluation .....</b>	<b>45</b>
5.1 Waveforms captured in significant operation modes.....	45

# 3 kW dual-phase LLC demo board

Using 600 V CoolMOS™ CDF7 and digital control by XMC4400

---

## Table of contents

5.2	Efficiency plot .....	49
<b>6</b>	<b>Conclusion .....</b>	<b>52</b>
<b>7</b>	<b>Technical Data Package (TDP) .....</b>	<b>53</b>
<b>8</b>	<b>Related resources .....</b>	<b>54</b>
<b>9</b>	<b>References .....</b>	<b>55</b>
<b>Glossary</b>	<b>.....</b>	<b>56</b>
<b>Revision history</b>	<b>.....</b>	<b>58</b>
<b>Disclaimer</b>	<b>.....</b>	<b>59</b>

### Introduction

## 1 Introduction

The combined trends of continuous reduction of volume and size of the power converters and increase of required output power represent a serious challenge in modern SMPS designs.

When addressing the HP density requirement, even in an SMPS with high peak efficiency, a typical problem is getting rid of the heat generated, especially at the full load, in the limited volume available.

A very powerful fan can help, but there may be a lot of side-effects, such as acoustic noise or vibration, which may be not tolerated by other system components, for example hard disk drives in computing applications. And in any case the effectiveness of the forced ventilation is linked to the air impedance inside the SMPS. Unfortunately, a typical consequence of the power density increase is the increase of the air impedance inside the PSU.

Especially in industrial and telecom applications, there are cases where the fan is not allowed.

The best solution is to try to limit the heat generated, especially under the most critical conditions from the thermal perspective: full-load operation. This means that having a very high peak efficiency (typically achieved at 50 percent load) may not be enough for the purpose, but the same high efficiency has to be extended up to full-load operation.

In other words, this requirement involves the need for a very flat efficiency plot, at least from 40–50 percent up to 100 percent load.

On the other hand, in N + 1 redundant application the percentage of SMPS operation near full load is lower than that below half-load, also making efficiency down to around 30 percent load important.

The combination of these typical performance requirements of industrial and telecom HP SMPS can be fulfilled through a very flat efficiency plot, from 30 percent to 100 percent load.

A similar curve is not compatible with the natural behavior of a power converter, whose efficiency plot is typically a parabola, with the peak at around mid-load. In other words, the desired “flatness” can be achieved only through a dedicated power converter design, which involves proper selection of topologies, power devices, magnetic components, and control techniques.

One of the most popular solutions adopted in power conversion in order to achieve this goal is the multi-phase approach. Scaling and balancing are two typical aspects of this design technique [15].

In this document the fundamental aspects of a Multi-phase LLC converter are analyzed, giving an overview of the most important design choices, especially in power semiconductors and control techniques.

A practical example is provided through the description of a 3 kW dual-phase LLC demo board designed entirely with Infineon power semiconductors and IC components.

This document shows the use of state-of-the-art HV and MV silicon MOSFETs, combined with optimized driving and sophisticated digital control to meet the most important requirements of a modern HP SMPS, both in terms of performance and reliability.

With the goal of achieving high reliability in the design, a prominent role is played in the analyzed topology by the HV MOSFET used in each HB LLC Converter. The selection of 600 V CoolMOS™ CFD7 SJ MOSFET provides all the benefits of the latest generation of fast body diode (BD) devices, able to guarantee reliable operation even in the critical operating modes of the multi-phase LLC topology.

All the features of the 600 V CoolMOS™ CFD7 technology are described in detail in [17], which complements this AN.

# 3 kW dual-phase LLC demo board

## Using 600 V CoolMOS™ CDF7 and digital control by XMC4400



### Dual-phase HB LLC design concept

## 2 Dual-phase HB LLC design concept

This application note provides a general overview of the Infineon 3 kW dual-phase LLC demo board and the concept behind it. Three important aspects of the present design are explained in this section. The specific control techniques used to address these three aspects will be explained in more detail in Section 4.

### 2.1 Current sharing and phase shedding

#### 2.1.1 The design challenges

The principle of operation of a single HB LLC converter is described in detail in [1].

Unlike a conventional PWM topology, based on a fixed frequency and variable duty cycle control, a resonant converter uses the switching frequency ( $F_{sw}$ ) as the main control parameter. The typical high gain of the resonant tank makes the resonant current ( $I_{res}$ ) very sensitive to the operating frequency.

When two resonant converters operate in parallel at the same frequency, any mis-match between the components of the two resonant tanks can generate a current imbalance in the two converters, which in the worst case can force all the current into one of the two phases, thus generating over-stress and most likely shut-down due to the Over Current Protection (OCP) mechanism.

A simulation performed with Simetrix on a dual-phase LLC circuit (Figure 1) clearly demonstrates the design challenges related to the current-sharing implementation.

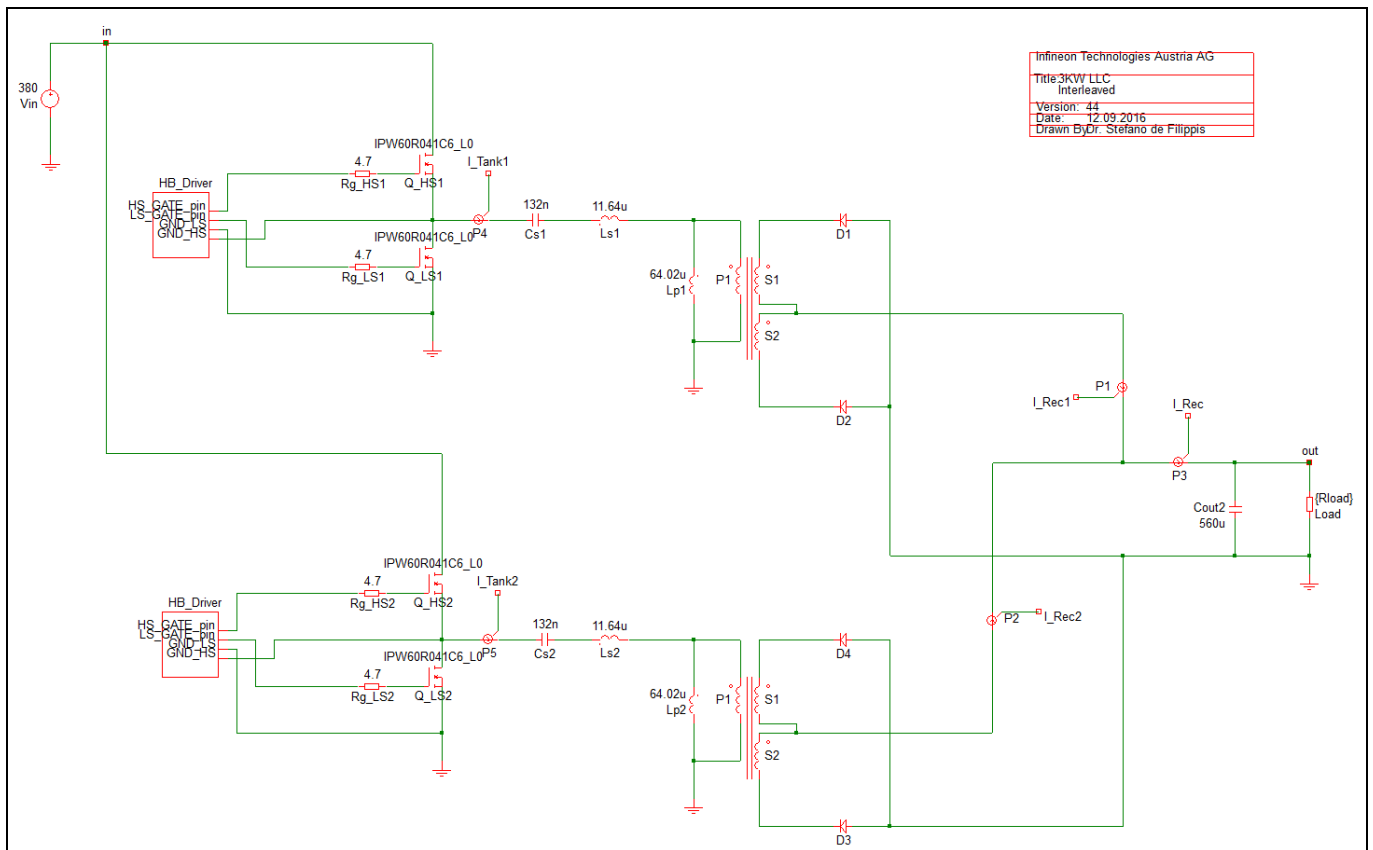


Figure 1 Simetrix simulation model of the 3 kW dual-phase LLC

Figures 2 and 3 (below) show the perfect balance of current in the two LLC converters, called Conv1 and Conv2 respectively, on both the primary and secondary side, in case of identical resonant tank components. The  $F_{sw}$  used for the simulations is the resonant frequency, which is the same for both converters. All the waveforms

# 3 kW dual-phase LLC demo board

Using 600 V CoolMOS™ CDF7 and digital control by XMC4400



## Dual-phase HB LLC design concept

(both primary and secondary) related to Conv1 are plotted in red; the ones related to Conv2 are plotted in green.

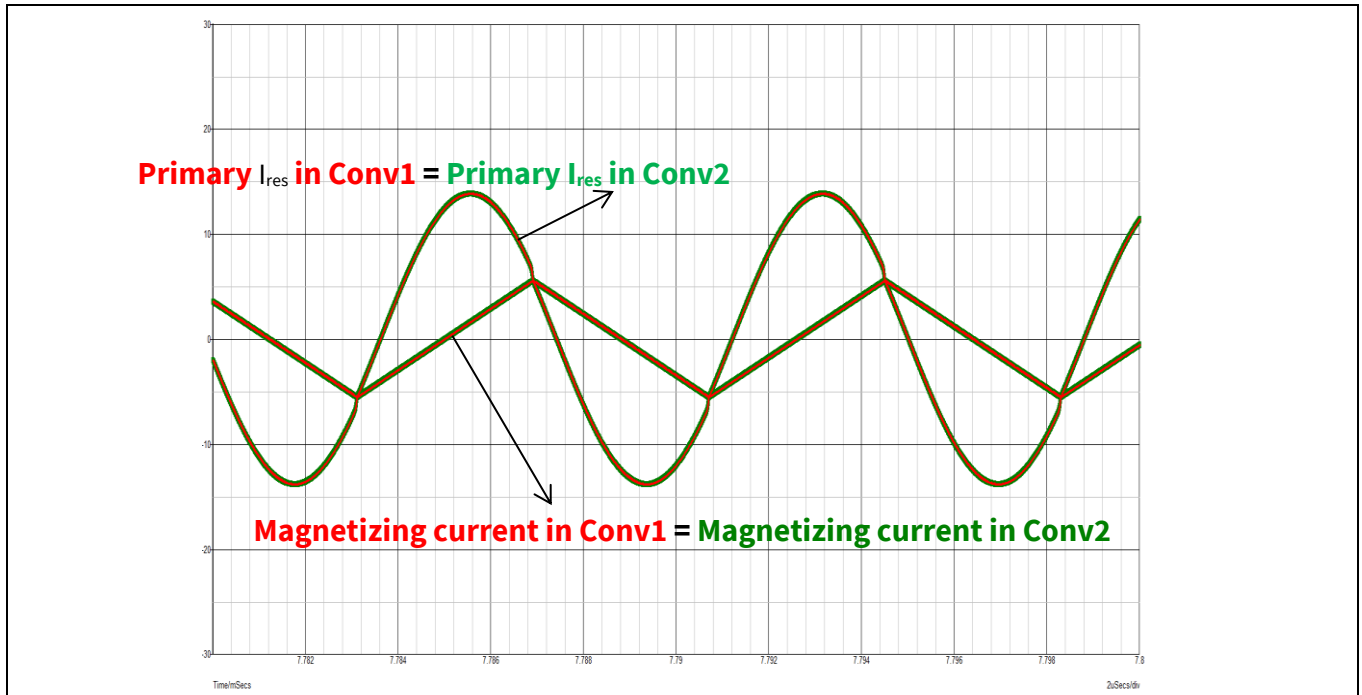


**Figure 2 Resonant and magnetizing currents in case of identical resonant tank components**

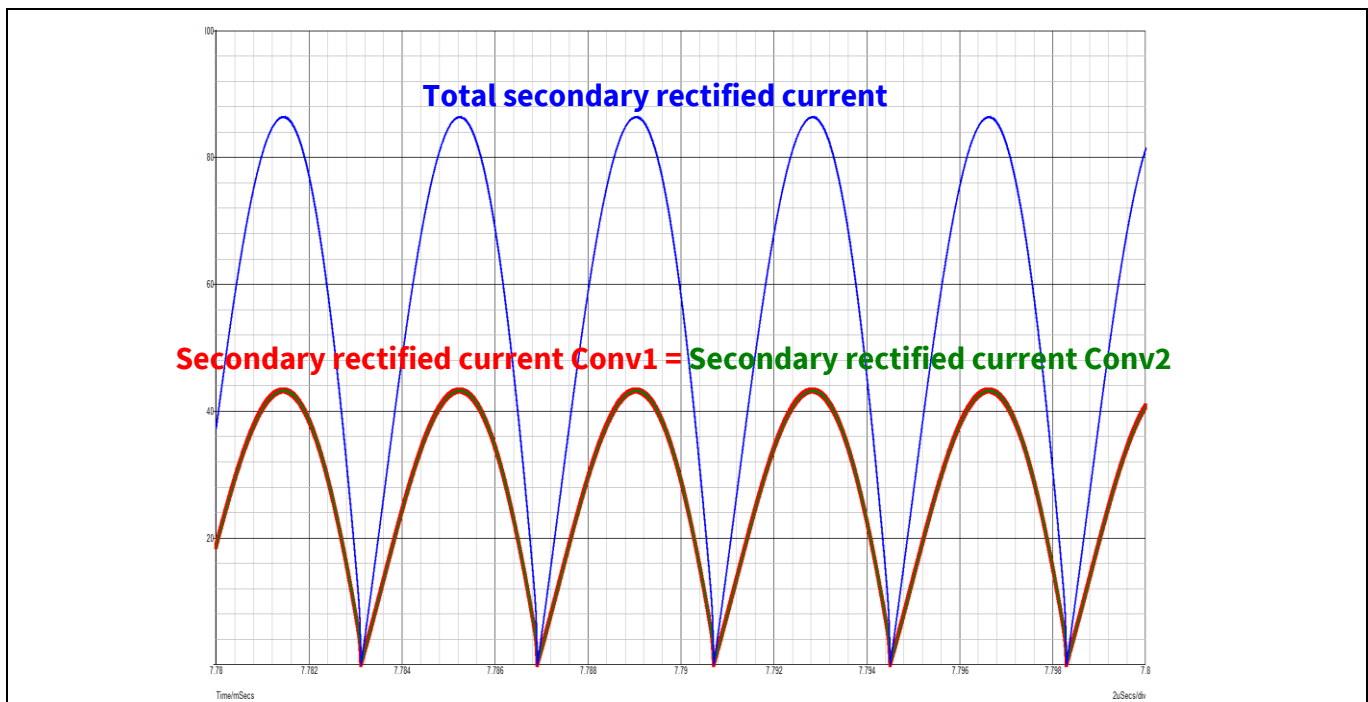


**Figure 3 Secondary rectified currents in case of identical resonant tank components**

From Figure 2 you can see that the primary resonant currents and, of course, the magnetizing currents are completely overlapping, as an obvious consequence of the perfect balance of the two phases, which should operate at the same resonant frequency. Figure 3 also shows that the secondary rectified currents are overlapping, and that each of them contributes by 50 percent to the full secondary rectified current, represented by the blue plot.

### Dual-phase HB LLC design concept

Figures 4, 5 and 6 refer to the case where there is a difference of only 5 percent between the values of the inductances in the two resonant tanks. Specifically, the resonant inductance ( $L_r$ ) in the Conv2 ( $L_{r2}$ ) is 5 percent smaller than the one in the other tank ( $L_{r1}$ ). This is a very common situation in practice, due to the typical tolerances in the range of  $\pm 10$  percent of the nominal values shown by this kind of magnetic component.

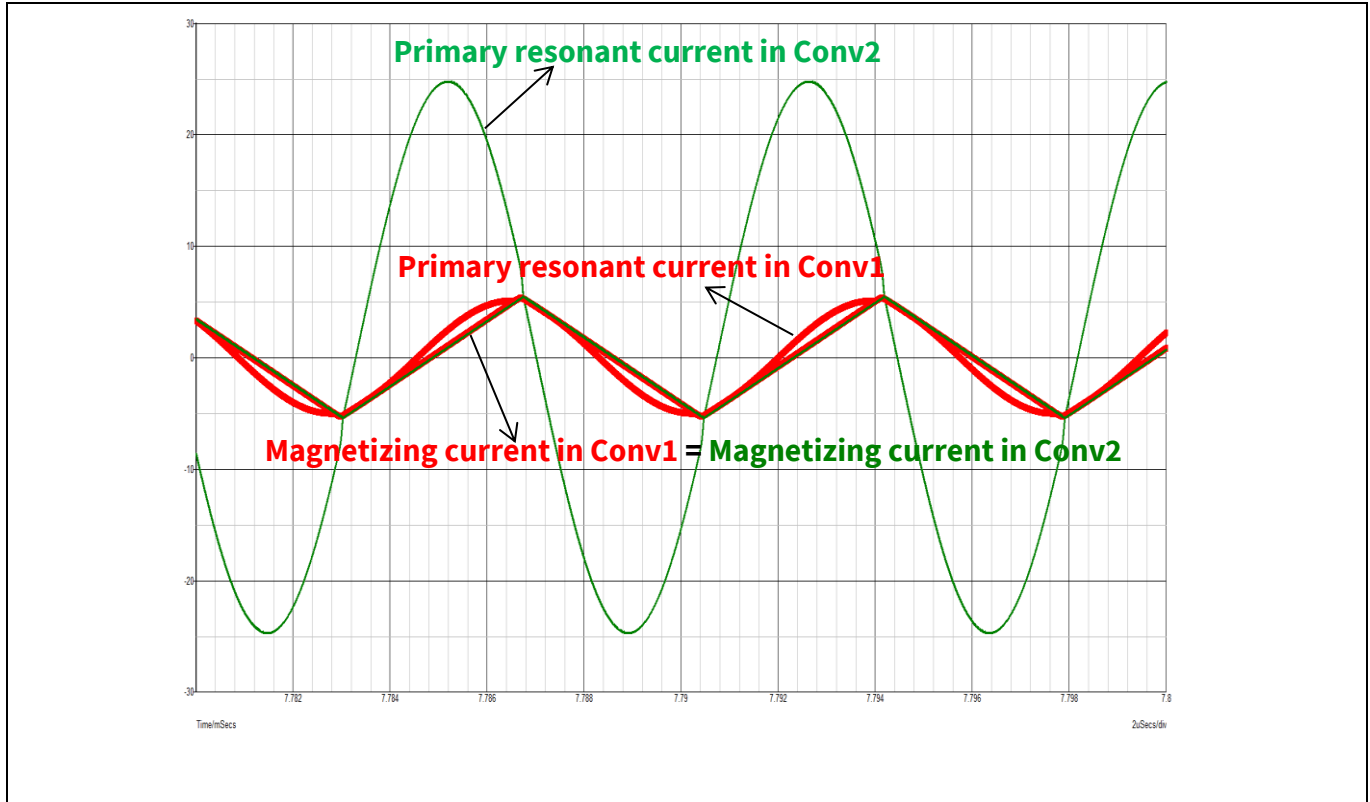


**Figure 4 Resonant and magnetizing currents in case  $L_{r2}$  is 5 percent smaller than  $L_{r1}$**

This small difference already generates a pretty high imbalance in the primary  $I_{res}$  of the two phases, as shown in Figure 4, while of course the two magnetizing currents are still perfectly coincident, since there is no change in the main transformers.

Basically, the reduction of  $L_{r2}$  generates a reduction in the equivalent impedance of the Conv2 resonant tank. Since the  $F_{sw}$  has been kept the same as in the balanced case, Conv2 shows a larger gain than Conv1 at this  $F_{sw}$ .

Figure 5 explains the reason for the Conv1 secondary rectified current shape in the case of  $L_r$  imbalance: the current is almost totally diverted into the Conv2 resonant tank, so the  $I_{res}$  in Conv1 becomes very low, almost overlapping the magnetizing current. In particular, during the time intervals when they are equal (e.g. starting from points 1 and 2 in Figure 5), the secondary rectified current becomes zero. This operation resembles the no-load operating condition and generates a secondary current in Conv1 similar to what it is expected in Discontinuous Current Mode (DCM) operation, typically seen when the LLC converters operate below resonance. Actually, the Conv1 still operates at the resonant frequency, since  $L_{r1}$  and  $C_{r1}$  have not been changed, but almost at no load, which is the reason why the secondary rectified current shows a discontinuous behavior.

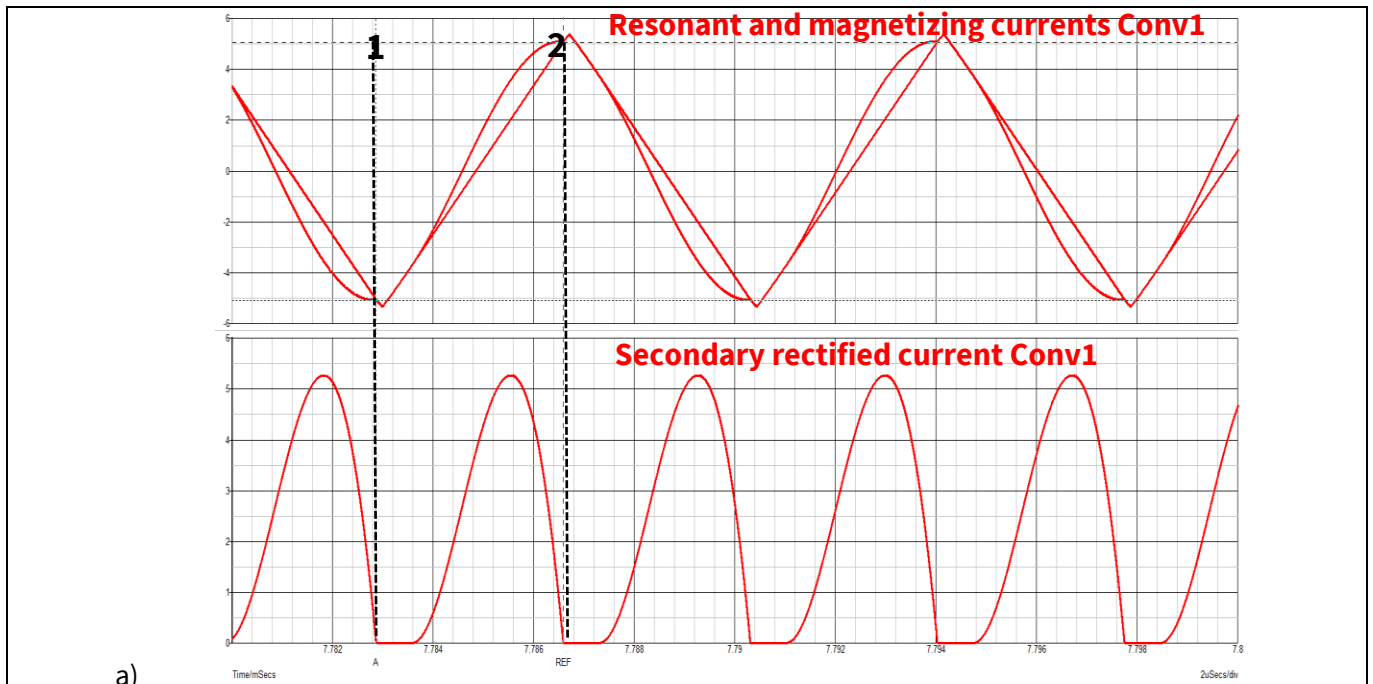


**Figure 5** Resonant, magnetizing, and secondary rectified currents in case  $L_{r2}$  is 5 percent smaller than  $L_{r1}$

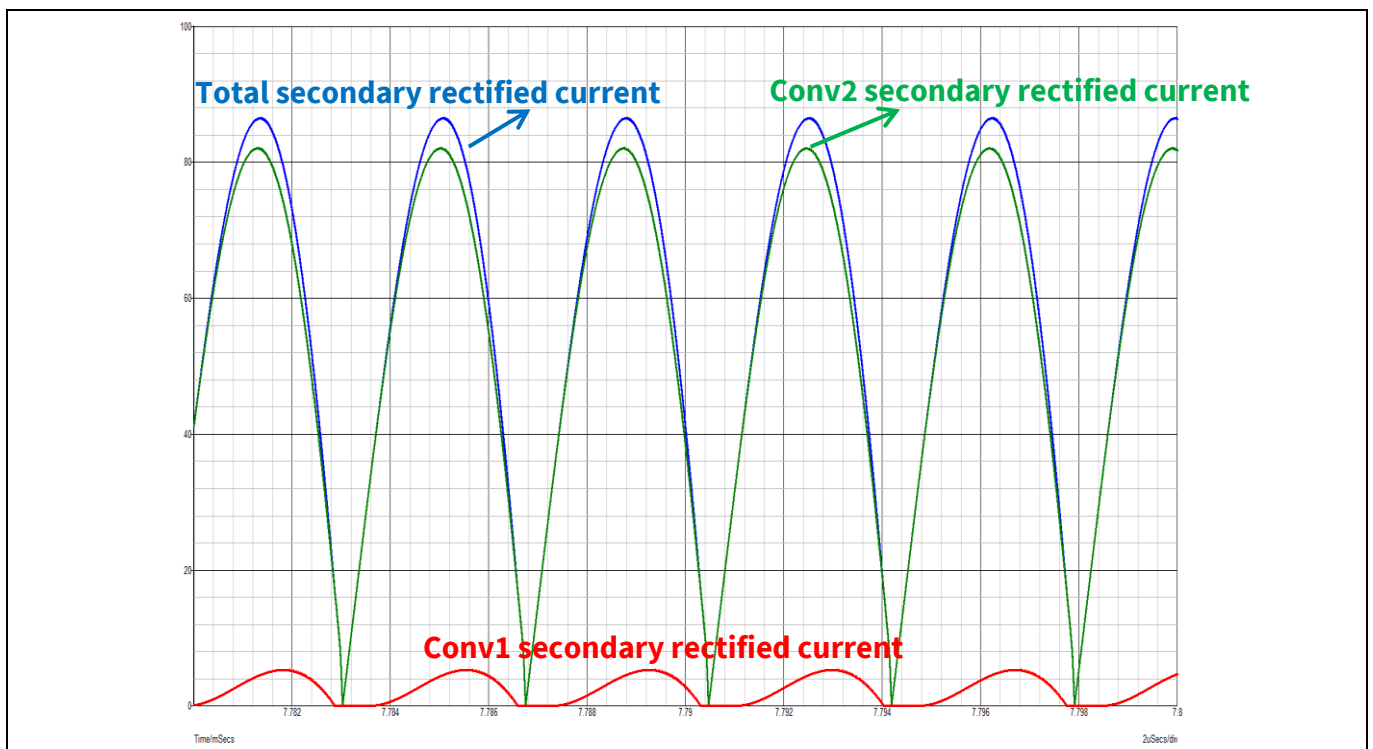


**Figure 6** Secondary rectified currents in case  $L_{r2}$  is 5 percent smaller than  $L_{r1}$

Looking at Figure 6, you can easily understand what happens in practice. The total secondary rectified current almost corresponds to the one in Conv2, which, in other words, will get almost the entire load current. Of course, the Conv2 is typically not designed to sustain the full load of the whole dual-phase converter, since it is supposed to work only up to half-load. Therefore, it will go immediately into output over-current/over-power, thus generating the shut-down of the complete converter.

#### Dual-phase HB LLC design concept

Further simulations show that a similar behavior can be observed in case of a mis-match of only 5 percent in the values of the resonant capacitors in the two HB LLCs.

These simple examples clearly demonstrate that the current sharing of two paralleled resonant converters is not a trivial topic and represents a real design challenge.

The technical literature suggests several techniques to avoid this issue.

The simplest is to perform a pre-selection of the resonant tank components (inductor and capacitor) in order to use identical values in the two phases. But this selection normally results in expensive and time-consuming SMPS mass production, especially for high volumes, so this solution is typically not chosen by big SMPS manufacturers.

A possible alternative solution is proposed in [2], where an additional intermediate conversion stage is added to regulate the LLC converter input voltage ( $V_{in}$ ) in order to allow each of the two converters to always operate at the optimal frequency for current balancing. The key to this technique is to get the output regulated through the variation of the  $V_{in}$  rather than the resonant stage gain. This solution avoids the current imbalance, but, on the other hand, will unavoidably impact the overall converter efficiency, due to the introduction of an additional conversion stage.

Another useful solution is proposed in [3] and [4]: it consists of compensating the resonant component mismatch by means of an additional inductor with an adjustable inductance value. In that approach the use of a magnetic core with saturation windings can provide an effective way of varying the value of the inductor wound on the same core. In order to be really effective, this technique requires a very precise output current measurement combined with a very accurate control of the resonant inductor value as a function of the current imbalance in two or more converter phases.

#### 2.1.2 Proposed implementation

Each of the methods described above has pros and cons.

In our 3 kW dual-phase design we opted for a more traditional direct control of the converter's  $F_{sw}$  as a function of the current in each of the two phases.

This technique also has several different implementations and, of course, several tricky aspects.

One of them is faced when trying to keep the two switching frequencies as close as possible. If they are very close but not exactly the same, this can result in beat frequency effects that can be critical for EMI and acoustic noise, as well as severely affecting the output ripple and thus requiring filtering. Some other techniques have the disadvantage of reducing the reliability and reproducibility of the resulting LLC converter arrangement.

In case the N-paralleled converters run at synchronized frequencies, having independent input voltages helps. However, this requires a separated PFC for each of the paralleled LLCs, which can increase the complexity of the PFC control. This solution does not give effective ratio efficiency vs cost and power density. Cost and power density are important considerations in modern high-power SMPS design.

In some cases, one converter is voltage controlled and the other (N-1) is current controlled, where the value used by the current controller is the output current of the voltage-controlled converter: a main drawback is that this can make the N LLC loops unstable.

Our 3 kW dual-phase LLC design concept is able to overcome the load imbalance between the two HB LLC converters while maintaining good reliability, reproducibility and efficiency.

The converter consists of two HB LLCs, each with its transformer, resonant choke and SR stage. A microcontroller located in the secondary side takes care of the control of both converters.

## 3 kW dual-phase LLC demo board

Using 600 V CoolMOS™ CDF7 and digital control by XMC4400



### Dual-phase HB LLC design concept

Figure 7 shows the general operational principle of the current sharing, by acting on the  $F_{sw}$  of one of the two converters. The so-called “phase shedding” function is also included, which consists of the switching-off one of the two converters below a certain load.

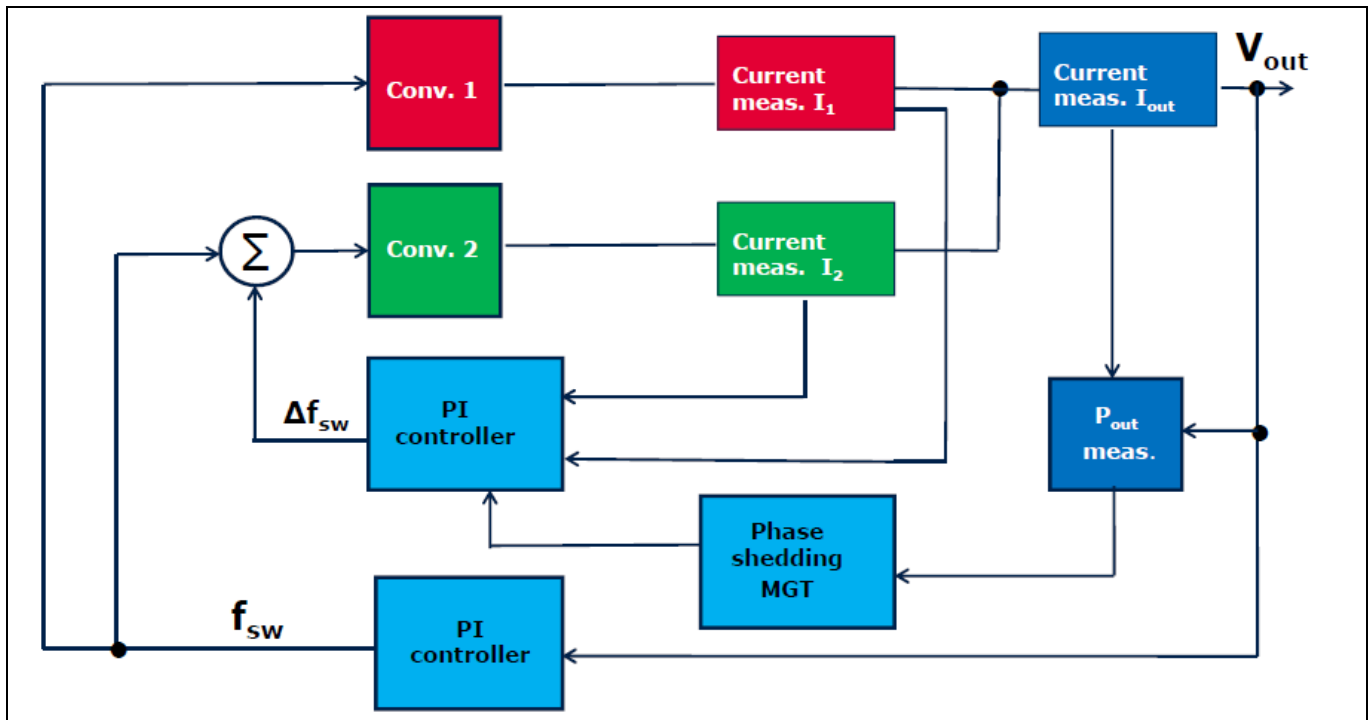


**Figure 7** General current-sharing principle of operation

In our approach, the two phases are treated separately, so the controller peripherals must accommodate the two phases' requirements in terms of PWMs and ADCs. The two converters may have parts tolerance/mis-match, resulting in different resonant frequencies; therefore, a separate PWM module is needed for each of the stages in order to modulate them separately to achieve current sharing.

The switching frequencies of the two LLCs are not the same, and the secondary current ripple cancelation is not guaranteed. The output ripple will increase until it reaches a maximum value when the two stages are in phase, then decreased until reaching a minimum value when the two stages are 90° out of phase. The ripple cancelation is in fact not in the main focus of our design, due to the relatively low output current (max. 55 A). Of course, the output current ripple reduction becomes more critical in the case of power converters with low output voltage ( $V_{out}$ ) and high output current: in those cases the interleaving by phase-shift of, the respective PWM paths is recommended.

The key concept of our control method is to split the output of the voltage controller into two or more control signals for the converters using the special balancing function. The balancing function is responsible for maintaining the highest efficiency in steady-state operation and prevents overloading of one of the two phases during quick power changes for dynamic regulation.

In Figure 8 you can find a schematic description of our implemented current-sharing method, which will be described in more detail in Section 4.

Dual-phase HB LLC design concept

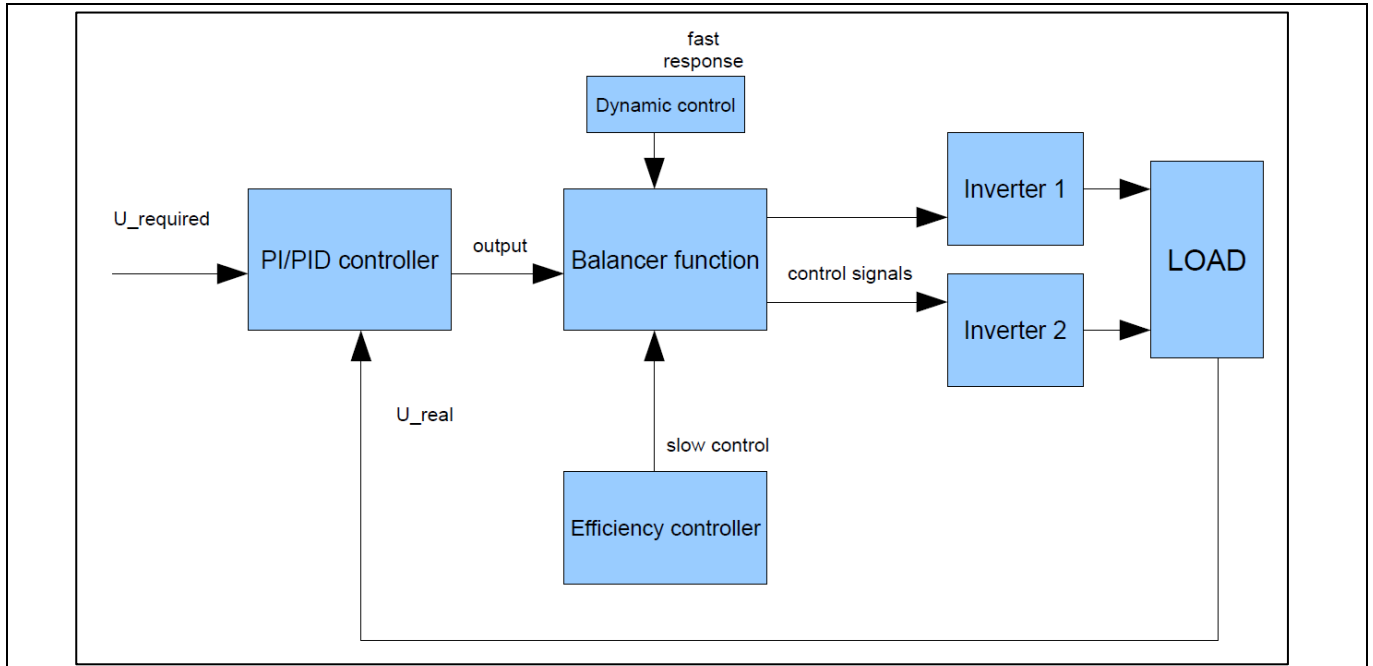


**Figure 8** Implemented current-sharing control

The implemented algorithm is also able to switch off one of the two phases below a certain output load, to guarantee a very flat efficiency plot across the entire load range. This technique is typically combined with current sharing among two or more converters working in parallel, and is known as phase shedding.

The importance of this feature is made clear in Figure 9, which shows the typical operating time distribution of an HP SMPS used in telecom or industrial applications.

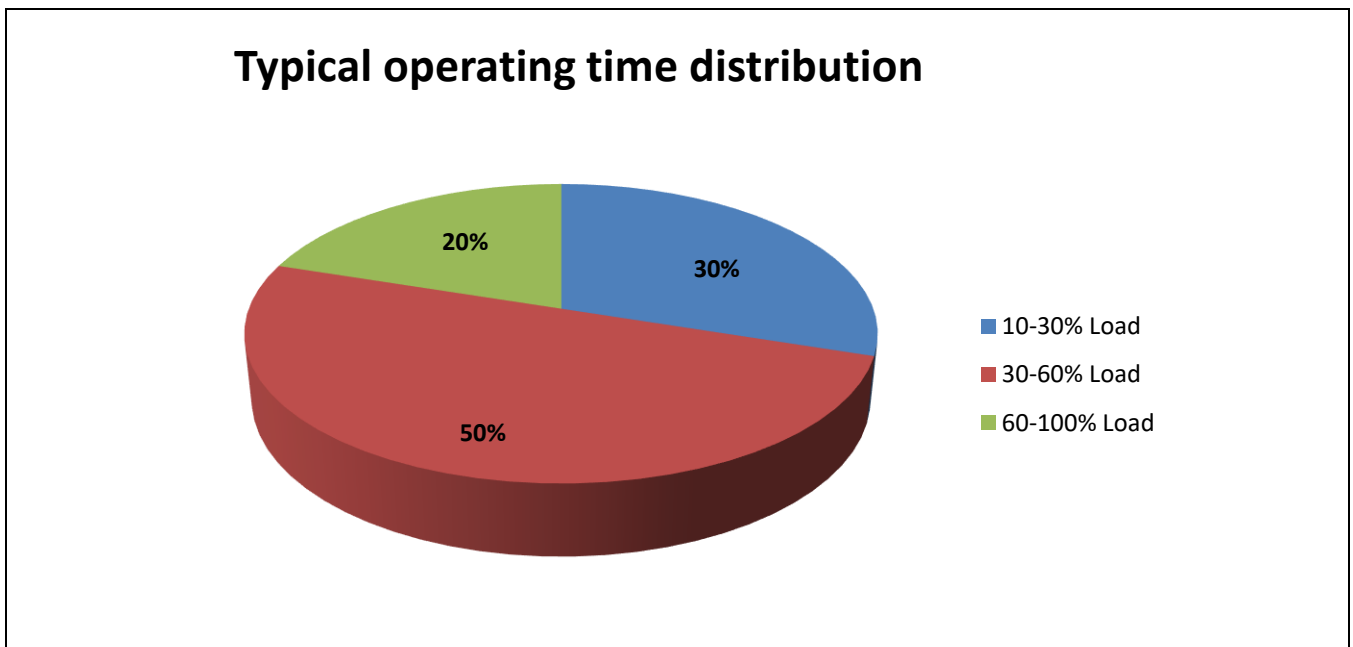


**Figure 9** Example of operating time distribution of a typical 3 kW power converter for telecom or industrial application

You can see that on average the most significant part of the operating time is spent in the 30–60 percent load range. The power supply also works for a considerable time in the 10–30 percent range, especially in an N + 1 redundant system.

## 3 kW dual-phase LLC demo board

### Using 600 V CoolMOS™ CFD7 and digital control by XMC4400

#### Dual-phase HB LLC design concept

The operation close to full load accounts for a relatively small part of the time: however, we know that this is the most critical part from a thermal perspective, so special care must be taken with it.

The multi-phase with phase-shedding approach addresses the requirements of high efficiency not only at mid-load (which is the “natural” behavior of a single-phase converter), but also a light and heavy load, making possible the aforementioned flatness of the efficiency plot.

The performance achieved in the present demo board is described in detail in Section 5 of this document. In that section you will see the crucial contribution of the power devices, especially the new 600 V CoolMOS™ CFD7 family, along with the control technique made possible by the XMC™ controller.

To complete the introduction to our concept and corroborate its effectiveness, Figure 10 shows the final efficiency plot achieved. You can see the very high peak efficiency, but also the very flat plot over the entire load range. The low driving and switching losses of the 600 V CoolMOS™ CFD7 technology are the key enablers of the very high efficiency at light load of each single HB LLC converter (or phase). The phase shedding is the other key contributor at light load. The flatness from medium to full load is the result of the excellent Figure of Merit (FOM)  $R_{DS(on)}$  \* switching losses of CFD7.

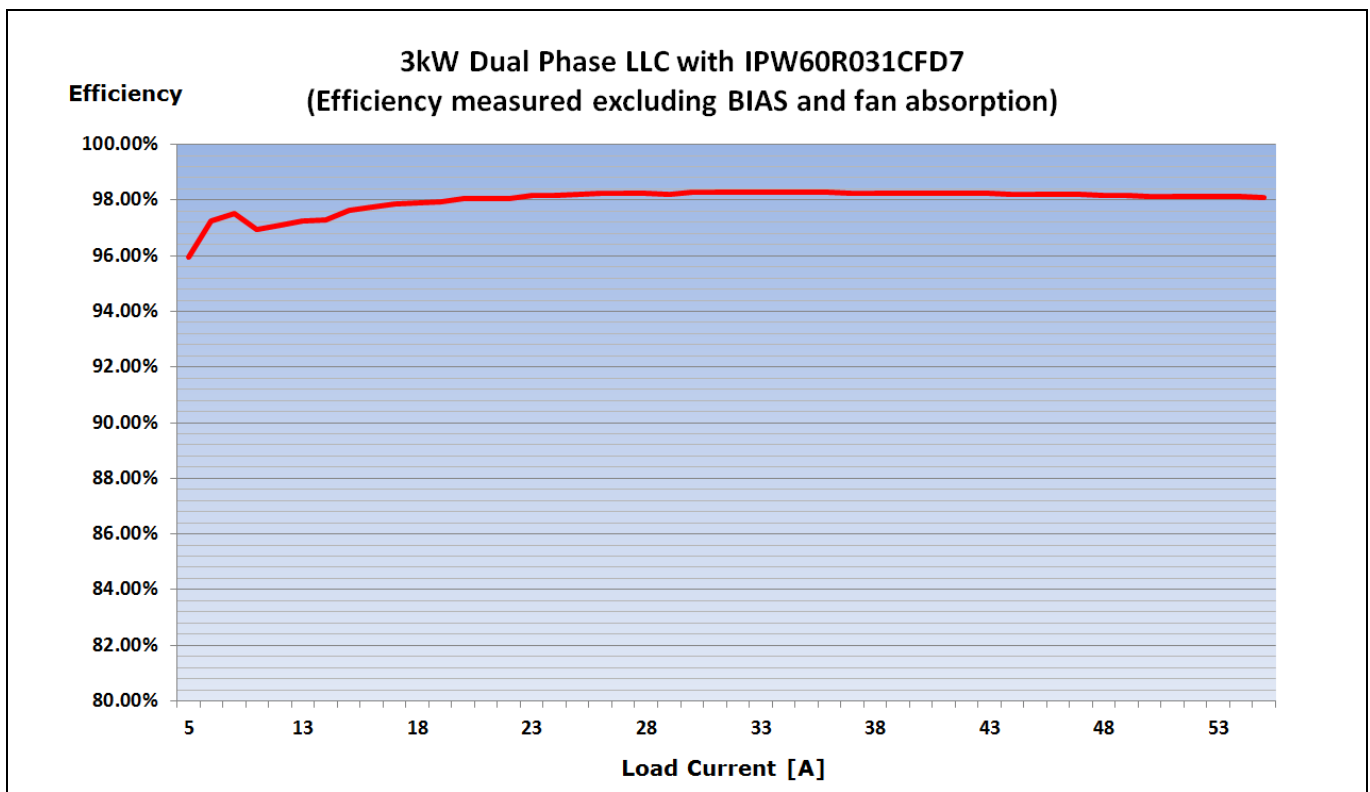


**Figure 10** 600 V CFD7-based 3 kW dual-phase LLC efficiency plot

## 2.2 Reliability features

The critical operating conditions of an HB LLC converter are well known in the SMPS designers’ community.

In fact, although knowledge of the HB LLC topology has significantly improved in the last 10 years, these critical operations often still discourage SMPS designers from using this solution for high-efficiency power converters where reliability matters. In fact, these conditions are considered particularly challenging, since they might occur in SMPS mass production, even in the field, despite the fact that this has never been reproduced in the lab tests during the design and qualification phase. Customers perceive this as extremely risky. Moreover, there are several studies showing that there is a huge difference in the cost of fixing an SMPS problem at different

### 3 kW dual-phase LLC demo board

#### Using 600 V CoolMOS™ CDF7 and digital control by XMC4400

#### Dual-phase HB LLC design concept

stages: e.g. the cost to fix it in the field/at the final customer site is 1000 times higher than during the design phase.

These tricky operating conditions of the HB LLC converter have already been analyzed in [1].

In a dual-phase approach, these problems are expected to be further amplified due to the synchronization of the two phases, which can be critical, especially during dynamic operation. So, special care must be taken with those aspects when designing LLCs in a multi-phase approach.

It is worth recapping the main problems that can occur in these critical operating conditions, before introducing the ways we avoid them in our 3 kW dual-phase LLC.

The best-known and most dangerous mechanism affecting LLC operation is the so-called hard-commutation on the conducting MOSFET BD. This typically occurs during the start-up sequence (illustrated in Figure 11), but also during burst mode or output short-circuit, and can lead to failure of the HV power devices in the primary side of the converter.

This problem occurs when one of the two MOSFETs in the HB LLC configuration (Q2 in Figure 11) is turned off while its BD is still not completely reverse-recovered. If this happens, when the other device (Q1) turns on, the MOSFET Q2 is submitted to heavy stress, since the  $V_{o,PFC}$  voltage is applied between its drain and source while a huge reverse current is flowing through the BD, creating a shoot-through effect. This stress can result in Q2 device failure, and Q1 may also be damaged. A very similar mechanism can be triggered during burst mode operation. The root cause of this behavior is the initial imbalanced voltage across the resonant capacitor, which leads to flux imbalance on the primary-side transformer.

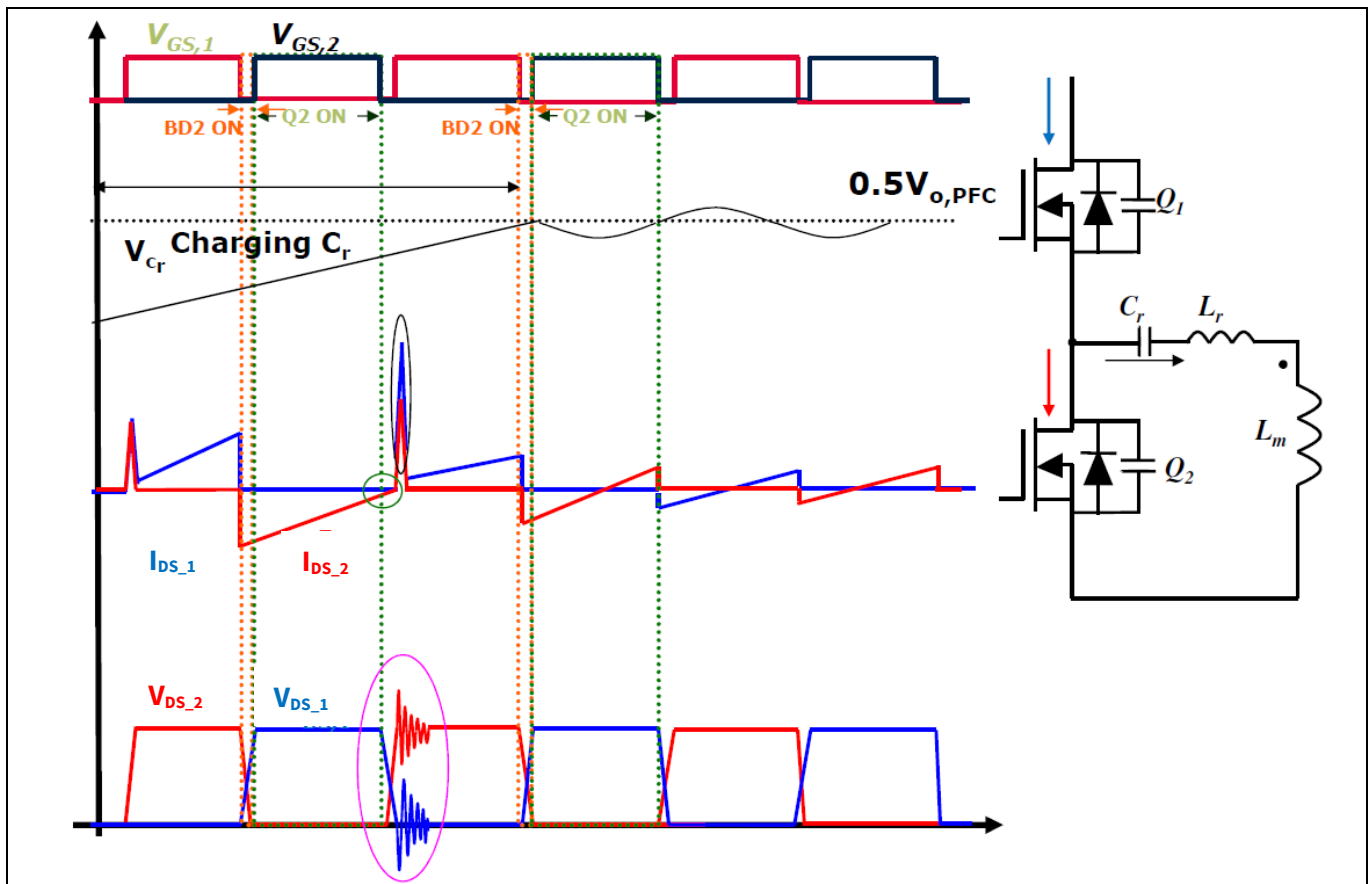


**Figure 11** Hard-commutation during HB LLC start-up sequence

## 3 kW dual-phase LLC demo board

### Using 600 V CoolMOS™ CDF7 and digital control by XMC4400

#### Dual-phase HB LLC design concept

Hard-commutation may also be experienced during load dump in conjunction with secondary-side Synchronous Rectification (SR): a feedback (FB) of energy from the secondary side to the primary side may occur, which leads to reversal of tank current and thus to hard-commutation on the primary MOSFETs.

In general, hard-commutation happens every time the  $I_{res}$  “leads” the resonant voltage, so that the voltage is in the mid-point of the HB: this specific condition is well known as “capacitive load mode operation” of the LLC converter.

There are several ways to prevent hard-commutation in the HB LLC topology. Some of them are “by design” (like the use of the so-called “split capacitor technique”). Actually it is impossible to precisely predict and avoid this condition by the converter design (e.g. LLC gain curves shape), without using a dedicated control strategy.

We decided to use a dedicated control strategy to prevent hard-commutation in all the possible triggering events, not only at start-up or in the case of output over-load, but in all those conditions, unpredictable by design, where the  $I_{res}$  may potentially “lead” the resonant voltage.

The proposed control is fully digital and is located on the secondary side, which has a couple of benefits in terms of transient response and output current measurement. The  $I_{res}$  is guaranteed to lag behind the resonant voltage: in fact the control is placed in the secondary side, but the primary-side tank current is continuously monitored by using a current transformer to provide the necessary reinforced isolation.

The start-up and burst mode sequences are based on the Zero Crossing Detection (ZCD) of the tank current, which is implemented totally inside the microcontroller without additional external hardware components (e.g. comparators). By detecting the tank current ZC the control ensures change of polarity of the tank current and thus current reversal in the main transformer. The four steps included in the start-up sequence are explained in detail in Section 4.

The algorithm implemented also includes an additional procedure that is able to detect load dump and prevent energy flow from the secondary side to the primary side. The control measures the output current and detects a negative slope in the measured current ( $-di/dt$ ), which indicates a fast decrease of load current. If a negative slope is detected, a dedicated SR control is applied.

Special care is needed in the management of the capacitive load mode condition, because this is recognized to be the most critical and often most unpredictable HV MOSFET failure mechanism in the LLC topology.

Our algorithm is able to both predict and protect against this. The control measures the phase-shift between the resonant voltage and  $I_{res}$ . Measurement for phase-shift can be implemented by counting the time from the MOSFET turn-off of the previous period until the tank current reverses (see Figure 12).

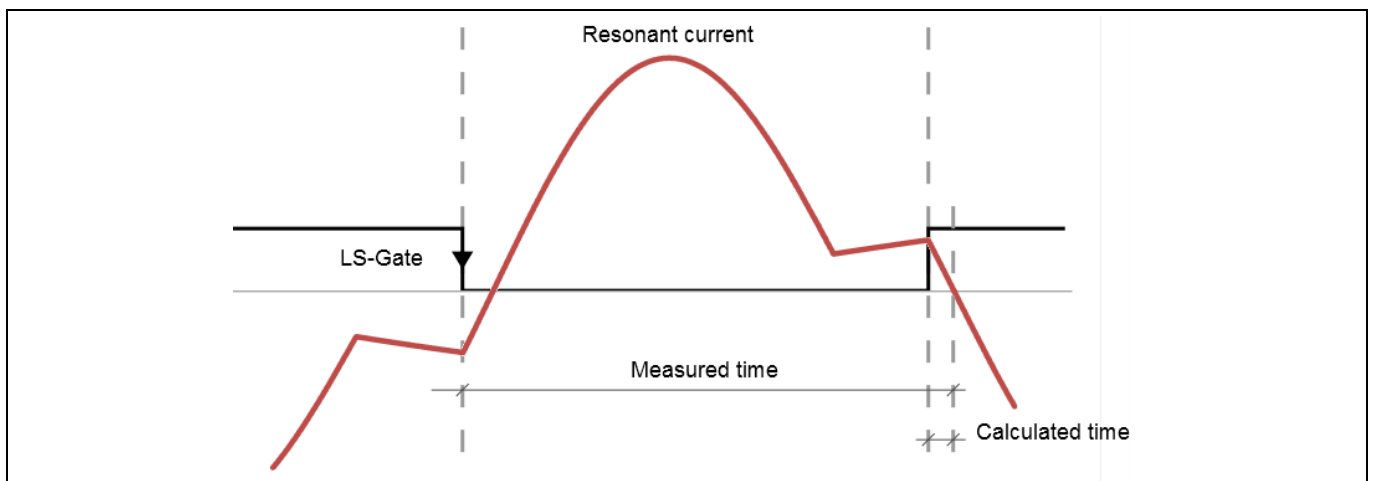


**Figure 12** Capacitive load mode prediction and protection concept

#### Dual-phase HB LLC design concept

The phase-shift is calculated from the measured time, dead time, and  $F_{sw}$ . If the phase-shift becomes zero, the operation point is close to the capacitive mode. The control increases  $F_{sw}$  to keep the operation point in the inductive region. This is the predictive or preventive feature implemented in our control. If a negative phase-shift is sensed, it means that capacitive mode has already occurred, and failure can be then prevented by simply turning off the MOSFET and not turning on the other MOSFET in the next half-cycle. The HB is also temporarily stopped as a precautionary measure to let the tank current decay to zero, and allow time for the switch node to bounce and the BD of the MOSFET to fully recover: this is the failure protection feature of our algorithm.

This paragraph has described the techniques implemented in the control of the 3 kW dual-phase LLC demo board in order to prevent/protect against hard-commutation on BDs that are not fully recovered. It has been shown [11] that this occurrence is more likely in HP converters, where MOSFETs with low  $R_{DS(on)}$  are used. As a general rule, devices with  $R_{DS(on)}$  less than 100 mΩ are more prone to this problem in LLC applications. In that case, an additional safety margin is provided by the use of a MOSFET with fast BDs, which physically minimizes the reverse minority current in the “shoot-through” effect described above, thus significantly reducing the risk of failure.

In conclusion, the combination of a device like the new CoolMOS™ 600 V CFD7 and the accurate control algorithms gives full confidence about the converter’s reliability, without sacrificing any performance.

### 2.3 Graphical User Interface (GUI)

A Graphical User Interface (GUI) has been designed as a complementary tool for the 3 kW dual-phase LLC design, with the purpose of enabling easy and intuitive interaction with the power converter.

The GUI enables the user to set some of the converter’s electrical parameters, such as the value of the  $V_{out}$ , maximum output current and the related OCP threshold.

Moreover, the GUI provides continuous monitoring of the converter’s operation, including  $V_{in}/V_{out}$  and current or temperature on the transformer of both phases. Several status and fault registers are visible, allowing for an immediate understanding of the reason for a fault condition.

The user may need to customize the operation of the board to their specific needs. For this reason the GUI makes it possible to re-configure the topology, e.g. by completely switching off one of the two phases, then limiting the maximum power to 1.5 kW. It is also possible to disable the SR stage, in case fine-tuning is required using only MOSFET BD rectification.

The GUI is able to automatically calculate the dead times as a function of the output capacitance ( $C_{oss}$ ) of the different MOSFETs used in the HB LLC: this enables design optimization according to the different MOSFETs used in the primary side, with the goal of guaranteeing ZVS behavior across the entire load range.

The user can also adjust the converter’s transfer function in order to optimize dynamic performance and loop stability.

The hidden and abstracted control concepts can be understood in a very precise and effective manner by means of a GUI. In fact, before the implementation of the control-loop design, a simulation is essential. This should prevent design problems arising during hardware implementation, when there will be limited room for maneuver. On the other hand, achieving an optimal response through simulation requires certain skills in control system theory; the precise positioning of poles and zeros in the compensator is not easy for less-experienced designers. Moreover, the loop compensation is also heavily influenced by the total amount of  $C_{oss}$ , including that applied outside the PSU. This additional capacitance often changes from case to case, even for the same PSU.

## 3 kW dual-phase LLC demo board

### Using 600 V CoolMOS™ CDF7 and digital control by XMC4400

---

#### Dual-phase HB LLC design concept

To help designers with this tedious part of their job, the GUI provides a menu where the total amount of additional external  $C_{oss}$  can be set, and then the algorithm will automatically re-calculate the poles and zeros of the transfer function for loop stability, by fulfilling the technical specification requirements:

Phase margin: min. 45° @ 0 bode plot gain crossover frequency

Gain margin: min. 10 db @ 0 bode plot phase crossover frequency

A more detailed description of the GUI functions is included in Section 4.8.

## 3 kW dual-phase LLC demo board

Using 600 V CoolMOS™ CDF7 and digital control by XMC4400

### Board description

## 3 Board description

The following sections provide an overview of the 3 kW dual-phase demo board, with details about the technical specifications, the electrical schematics, and the main active and passive components, including Infineon power devices and ICs, and magnetic parts.

### 3.1 Main requirements in the technical specification

- $V_{in}$  range 350 V<sub>DC</sub> to 410 V<sub>DC</sub>
- Nominal  $V_{in}$  380 V<sub>DC</sub>
- $V_{out}$  44 V to 58 V  $\pm$ 1 percent
- Nominal  $V_{out}$  54 V<sub>DC</sub>
- Max. output current/power 55 A/3000 W
- Dual-phase approach
- Power density > 30 W/inch<sup>3</sup>
- Efficiency target: 10/50/100 percent  $P_{max}$  = 95 percent /98 percent /97.5 percent

### 3.2 General overview of the final design

Figure 13 shows the basic structure of the 3 kW dual-phase LLC design.

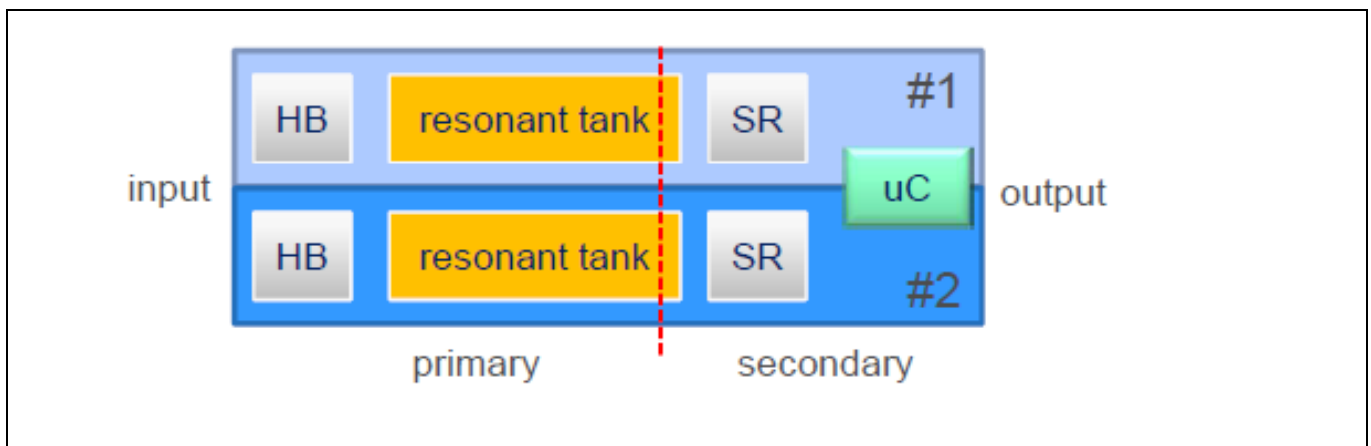


**Figure 13 3 kW dual-phase LLC: basic concept**

The board consists of two HB LLC converters working in parallel: each of them has its own resonant tank and SR stage. For the sake of simplicity, we will call these converters Conv1 and Conv2, as in the simulation described in the previous section. A single microcontroller located in the secondary side controls both converters. It generates the PWM signals for both primary and secondary MOSFETs and manages the current sharing and all the advanced features, which will be analyzed in depth in Section 4.

Figure 13 shows a real picture of the 3 kW dual-phase LLC demo board and highlights the position of the most significant components, including of course the Infineon products used.

A main power board and two daughter cards are visible in Figure 14. In the main board all the power components are assembled, including MOSFETs and magnetic parts. The first daughter card hosts the microcontroller and the related logic circuitry, so this is identified as the control card. The second daughter board (bias card) hosts the auxiliary converter, which is done with a QR Flyback converter: as is typical in HP SMPS, this small converter provides the voltages needed to supply the logic circuitry and the two ventilators, also visible in Figure 14.

## 3 kW dual-phase LLC demo board

### Using 600 V CoolMOS™ CFD7 and digital control by XMC4400

#### Board description

Section 3.3 gives an overview of the Infineon components that have been used in the present design, highlighting their main features. Section 3.4 will go into the details of the electrical schematics and the magnetic component specifications.

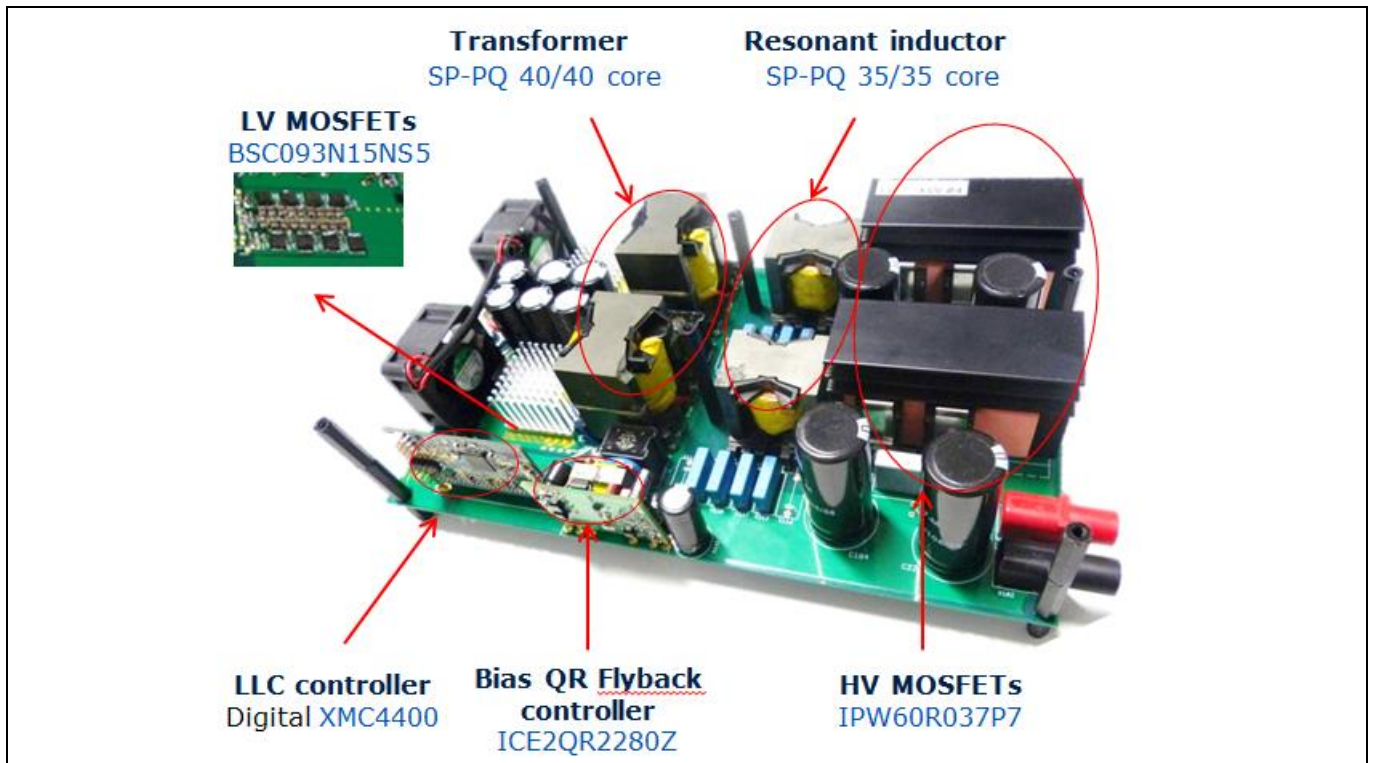


**Figure 14** The 3 kW dual-phase LLC demo board

## 3.3 Infineon components

### 3.3.1 Primary HV MOSFETs 600 V CoolMOS™ CFD7

CoolMOS™ is a revolutionary technology for HV power MOSFETs, designed according to the SJ principle and pioneered by Infineon Technologies. The latest CoolMOS™ CFD7 is the successor to the CoolMOS™ CFD2 series, and is an optimized platform tailored to target soft-switching applications such as phase-shift full-bridge (FB) ZVS and LLC. Resulting from reduced gate charge ( $Q_g$ ), best-in-class reverse recovery charge ( $Q_{rr}$ ) and improved turn-off behavior, CoolMOS™ CFD7 offers the highest efficiency in resonant topologies. As part of Infineon's fast body diode portfolio, this new product series blends all advantages of a fast-switching technology together with superior hard-commutation robustness, without sacrificing easy implementation in the design-in process. The CoolMOS™ CFD7 technology meets the highest efficiency and reliability standards and also supports high power density solutions. Altogether, CoolMOS™ CFD7 makes resonant switching topologies more efficient, more reliable, lighter, and cooler.

#### Features:

- Ultra-fast BD
- Low gate charge
- Best-in-class reverse recovery charge ( $Q_{rr}$ )
- Improved MOSFET reverse diode  $dv/dt$  and  $di/dt$  ruggedness
- Lowest FOM  $R_{DS(on)} * Q_g$  and  $R_{DS(on)} * E_{oss}$
- Best-in-class  $R_{DS(on)}$  in SMD and THD packages

## 3 kW dual-phase LLC demo board

### Using 600 V CoolMOS™ CDF7 and digital control by XMC4400

#### Board description

- Qualified for industrial-grade applications according to JEDEC (J-STD20 and JESD22)

#### Benefits:

- Excellent hard-commutation ruggedness
- Highest reliability for resonant topologies
- Highest efficiency with outstanding ease-of-use/performance trade-off
- Enabling increased power density solutions

#### Applications:

- Suitable for soft-switching topologies
- Optimized for phase-shift FB (ZVS), and LLC stages in server, telecom, and EV charging applications

### 3.3.2 Isolated gate drive 1EDI60N12AF

The Infineon EiceDRIVER™ 1EDI Compact family consists of a single-channel HV gate driver IC with integrated Coreless Transformer (CLT) technology and a maximum offset voltage of 1200 V. The 1EDI Compact driver ICs are available in a compact PG-DSO-8 (150 mil) package and provide either separated source/sink outputs or a single output with an additional clamping function.

Summary of the 1EDI60N12AF features:

- Separate source/sink output
- $I_{out}$ : 6 A @ 15 V
- 1200 V Coreless Transformer IC with galvanic isolation
- Prop. delay < 105 ns with 40 ns input filter time
- High CMTI robustness > 100 V/ns

#### Benefits:

- Tailored to all 600 V CoolMOS™ CFD7 and P6 families, and in general for SJ MOS transistors
- High  $F_{sw}$  applications such as SMPS, up to 4 MHz
- Turn-off vs turn-on fine-tuning
- High reliability at small footprint

In the present demo board, the 1EDI60N12AF is used to drive the High-Side (HS) and Low-Side (LS) MOSFETs of each of the two HB LLCs. Its reduced propagation delay is an important feature in our application due to the microcontroller position on the secondary side; moreover, the high CMTI and the possibility of split-source and sink outputs help to get the full benefit out of the 600 V CoolMOS™ CFD7 switching behavior.

### 3.3.3 SR MOSFETs OptiMOS™ BSC093N15NS5

The OptiMOS™ 5 150 V dramatically improved the  $R_{DS(on)}$  per package for this voltage range: 9.3 mΩ is available even in the compact Super SO8 package, which has been used in the present demo board. This enables the customer to switch from the FB SR topology on the secondary side to the center-tap transformer approach, yielding simplicity in the design and cost reduction (only simple LS drivers needed instead of two HB drivers).

This is in fact the main reason why we opted for a center-tapped transformer in the present 3 kW LLC design despite the relatively high  $V_{out}$ .

The OptiMOS™ 5 150 V has a more linear  $C_{oss}$ , and yet there is a reduced total output charge in comparison with the previous generation: this contributes to reducing any voltage overshoot.

## 3 kW dual-phase LLC demo board

### Using 600 V CoolMOS™ CDF7 and digital control by XMC4400

#### Board description

The BD has increased ruggedness due to the reduced  $Q_{rr}$  offered by the new technology: these results in reduced overshoot when the converter operates above resonance and during abnormal conditions.

Finally, the typical OptiMOS™ 5 technology very tightly matches some key parameters, like  $V_{GS,th}$ , which is a fundamental feature in order to guarantee a reliable SR operation, especially in a dual-phase design, where each of the phases also uses several paralleled devices in each branch.

#### 3.3.4 Advanced dual-channel gate drive 2EDN7524

The fast dual-channel 5 A non-isolated gate driver is an advanced dual-channel driver optimized for both standard and SJ MOSFETs, as well as GaN power devices, in all applications in which they are commonly used. The input signals are TTL compatible with an HV capability up to 20 V and down to -5 V. The unique ability to handle -5 V<sub>DC</sub> at the input pins protects the IC inputs against GND-bounce transients.

Each of the two outputs is able to sink and source current up to 5 A, utilizing a true rail-to-rail stage that ensures very low impedances of 0.7 Ω up to the positive and 0.55 Ω down to the negative rail. Very low channel-to-channel delay matching (typically 1 ns) is implemented, which enables the double source-and-sink capability of 10 A by paralleling both channels.

Different logic input/output configurations guarantee high flexibility for all applications; e.g. with two paralleled switches in a boost configuration. The gate driver is available in three package options: PG-DSO-8, PG-VDSO-8 and PG-TSDSO-8-X (size minimized DSO-8).

In the present demo board, the 2EDN7524 is used to drive the SR MOSFETs. In this application the 5 A peak current capability and the very precise channel-to-channel delay matching, along with the high reverse current capability and negative input capability, are beneficial features in order to guarantee an SR-efficient but also reliable operation. In fact the reliability and perfect delay time matching aspects are very important in the complex SR management inside a dual-phase LLC design.

#### 3.3.5 XMC4400 microcontroller

The XMC4400 combines Infineon's leading-edge peripheral set with an industry-standard ARM® Cortex®-M4F core.

The control of SMPS is a strong focus for XMC™ microcontrollers, where users can benefit from features such as smart analog comparators, High Resolution (HR) PWM timers and the ARM® Cortex®-M4F DSP instruction set, including floating-point or high-precision ADCs.

As a key feature it offers an HRPWM unit with a resolution of 150 ps. This unique peripheral makes it especially suitable for digital power conversion in applications such as solar inverters as well as SMPS and Uninterruptible Power Supplies (UPS). The XMC4400 is supported by Infineon's integrated development platform DAVE™, which includes an IDE, debugger and other tools to enable a fast, free-of-charge, and application-orientated software (SW) development.

Summary of XMC4400 features:

- ARM® Cortex®-M4F, 120 MHz, incl. single-cycle DSP MAC and floating point unit (FPU)
- 8-channel DMA + dedicated DMA for USB
- CPU frequency: 120 MHz
- High ambient temperature range: -40°C to 125°C
- Wide memory size options: up to 512 kB of Flash and 80 kB of RAM
- HRPWM, allowing PWM adjustment in steps of 150 ps
- 12-bit ADC, 2 MSample/sec. flexible sequencing of conversions including synchronous conversion of different channels

#### Board description

- Fast and smart analog comparators offer protections such as overcurrent protection, including filtering, blanking, and clamping of the comparator output. A 10-bit DAC with a conversion rate of 30 MSamples/sec provides an internal reference for the comparators that can be configured to be a negative ramp for slope compensation purposes
- A flexible timing scheme due to CCU timers and HRPWM (High Resolution PWM). These timers allow the creation of almost any PWM pattern and synchronize PWM signals with ADC measurements accurately
- Interconnection matrix to route different internal signals from one peripheral to another. For example, the comparator output can connect to a PWM timer to indicate an OCP event and immediately switch off the PWM output
- Communication protocols supported include USB, UART, I<sup>2</sup>C, SPI
- USB 2.0 full-speed device
- Package: PG-LQFP-64

#### 3.3.6 Bias QR Flyback controller ICE2QR2280Z

ICE2QRxxxx is the second-generation quasi-resonant PWM CoolSET™ with power MOSFET and start-up cell included in a single-package optimized for off-line power supply applications such as LCD TVs, notebook adapters and auxiliary/housekeeping converters in SMPS. The digital frequency reduction with decreasing load enables a quasi-resonant operation down to a very low load. As a result, the average system efficiency is significantly improved compared to conventional solutions. The active burst mode operation enables ultra-low power consumption during standby mode operation, and low  $V_{out}$  ripple. The numerous protection functions give full protection of the power-supply system in potential failure situations.

In the 3 kW demo board the ICE2QR2280Z is used in the auxiliary converter, which has the task of generating all the voltages supplying logic circuitry and ventilators.

The key features of the ICE2QR2280Z for use as an auxiliary converter of this LLC evaluation board are:

- HV (800 V) avalanche rugged CoolMOS™ with start-up cell
- Quasi-resonant operation
- Load-dependent digital frequency reduction
- Active burst mode for light load operation
- Built-in HV start-up cell
- Built-in digital soft-start
- Cycle-by-cycle Peak Current Limitation (PCL) with built-in Leading Edge Blanking (LEB) time
- Foldback point correction with digital sensing and control circuits
- $V_{CC}$  Under Voltage (UV) and overvoltage (OV) protection, with auto-restart mode
- Over-load/open-loop protection with auto-restart mode
- Built-in overtemperature protection with auto-restart mode
- Adjustable output overvoltage protection with latch mode
- Short-winding protection with latch mode
- Maximum on-time limitation
- Maximum switching-period limitation

# 3 kW dual-phase LLC demo board

Using 600 V CoolMOS™ CDF7 and digital control by XMC4400



## Board description

### 3.4 Board schematics

#### 3.4.1 LLC switching power stage

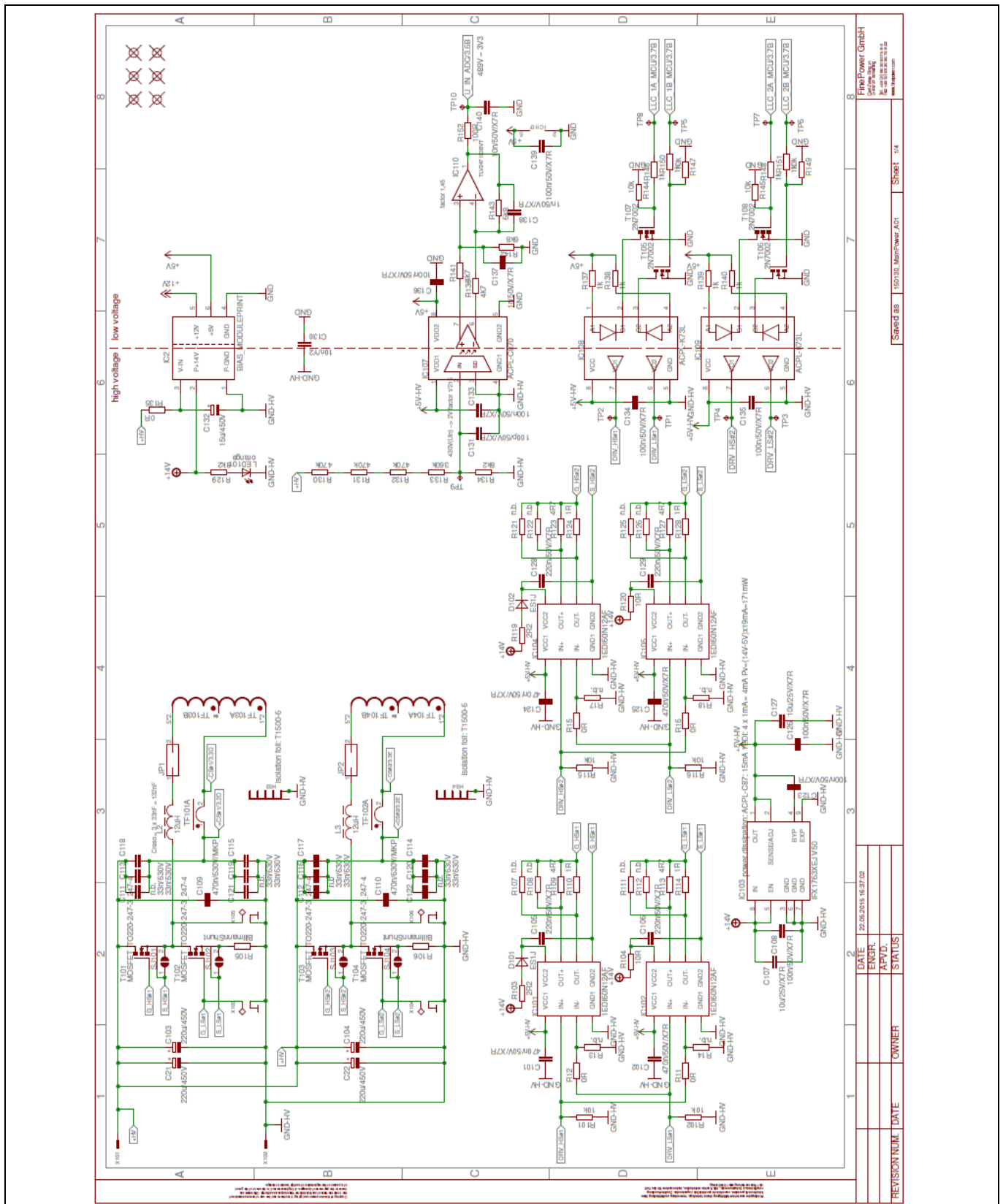


Figure 15 Primary HV power stage

# 3 kW dual-phase LLC demo board

Using 600 V CoolMOS™ CDF7 and digital control by XMC4400



## Board description

### 3.4.2 Synchronous rectification and secondary stage

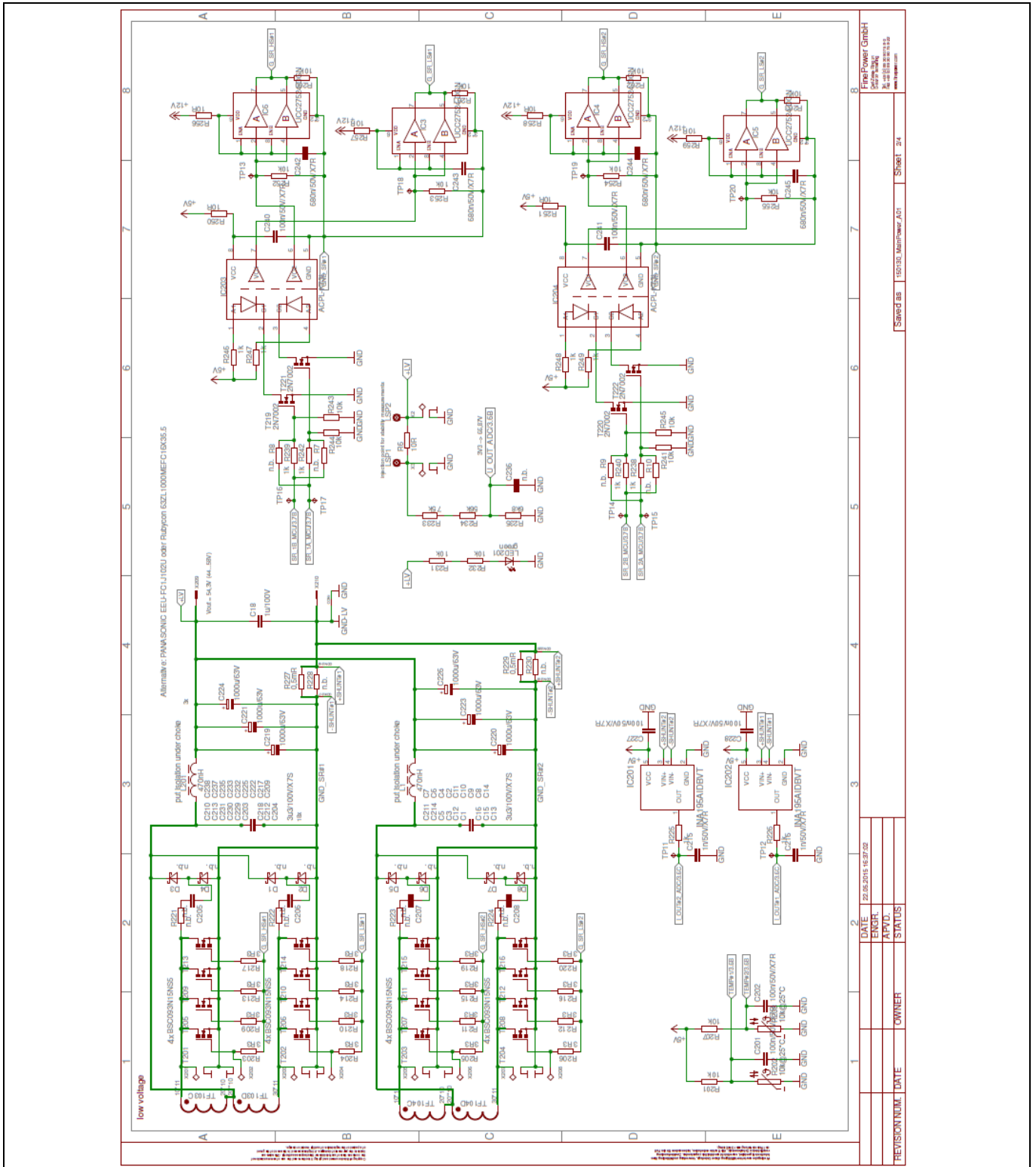
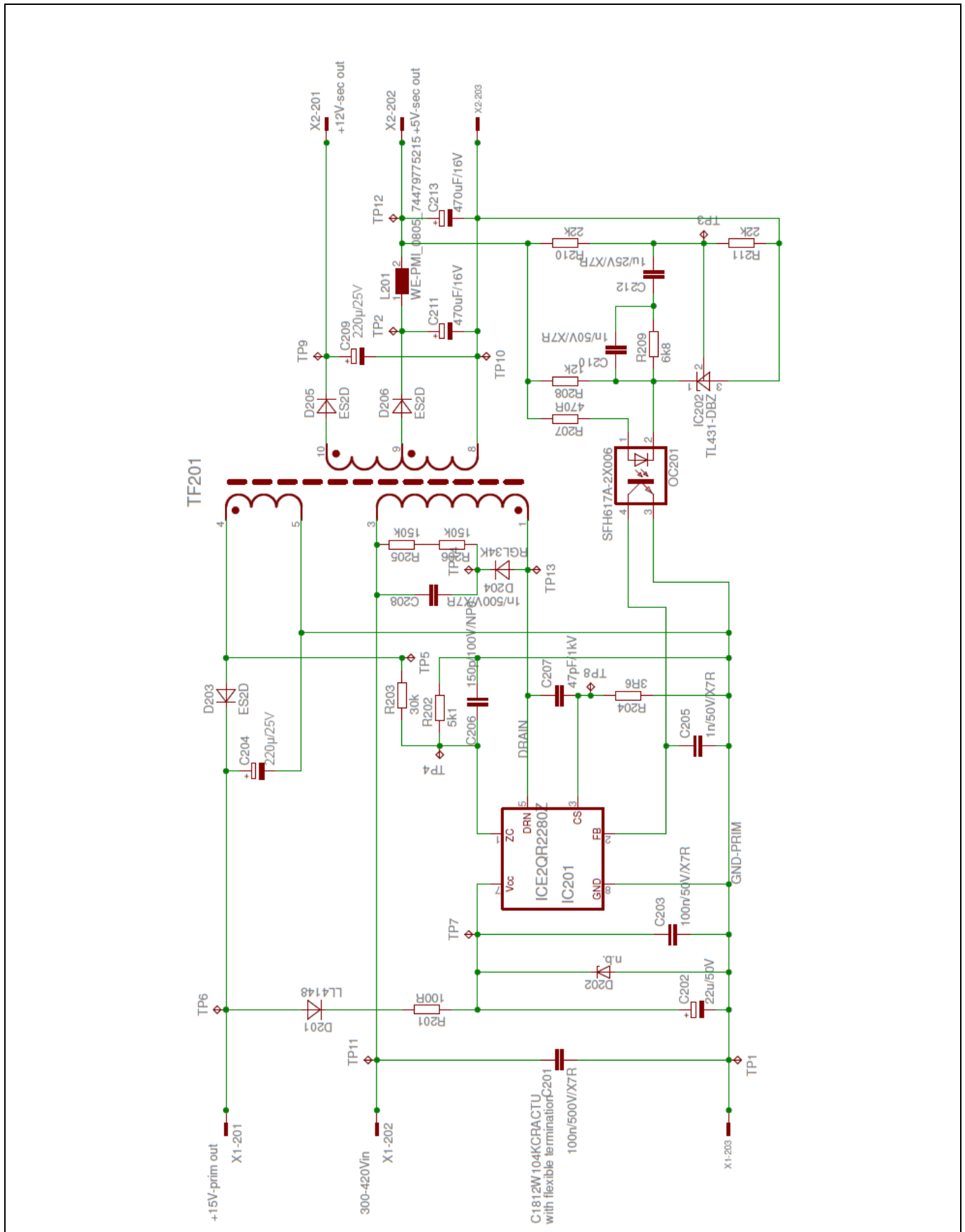


Figure 16 Secondary-side power stage



### Board description

#### 3.4.4 Bias board (auxiliary converter)



**Figure 18** QR Flyback auxiliary converter

# 3 kW dual-phase LLC demo board

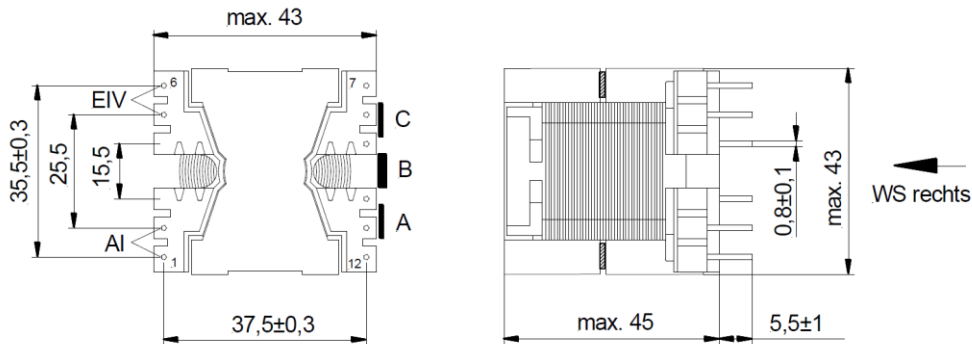
Using 600 V CoolMOS™ CDF7 and digital control by XMC4400



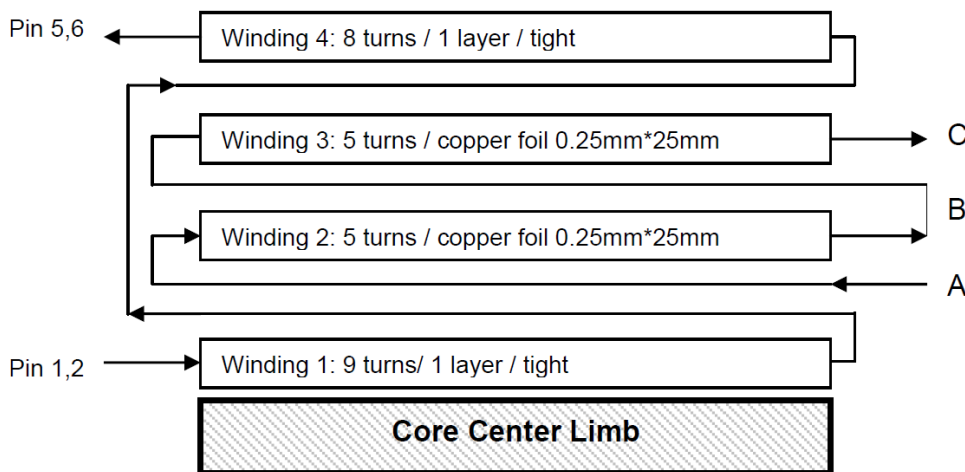
## Board description

### 3.5 Magnetic components

#### 3.5.1 HB LLC main transformer



Core form and material	PQ40/40, N95
Bobbin	Epcos, B65884E0012D001
Primary inductance $L_p$	78uH, measured between 1,2 and 5,6, other pins open
Airgap	Distributed air gap on all three limbs
Leakage inductance $L_{lk}$	0.5uH, measured between 1,2 and 5,6, other pins shorted
Isolation voltage $V_{iso}$	2500V <sub>rms</sub> / 50Hz, 1min (between 1,2,3,4,5,6 and A,B,C)



Windings	Start	End	Wire	Turns	Layers	Method
1	1,2	3 or float	60x0.2mm Litz or 2 times 30x0.2mm Litz	9	1	Tight
2	A	B	0.25mm*24mm copper foil	5	1	Tight
3	B	C	0.25mm*24mm copper foil	5	1	Tight
4	4 or float	4,5,6	60x0.2mm Litz or 2 times 30x0.2mm Litz	8	1	Tight

The transformer is produced by Infineon’s trusted partners in the development and manufacturing of magnetic components:

- [Kaschke Components GmbH](#) – Göttingen, GERMANY
- [ICE Transformers s.r.l.](#) – Loreto Aprutino (Pescara), ITALY

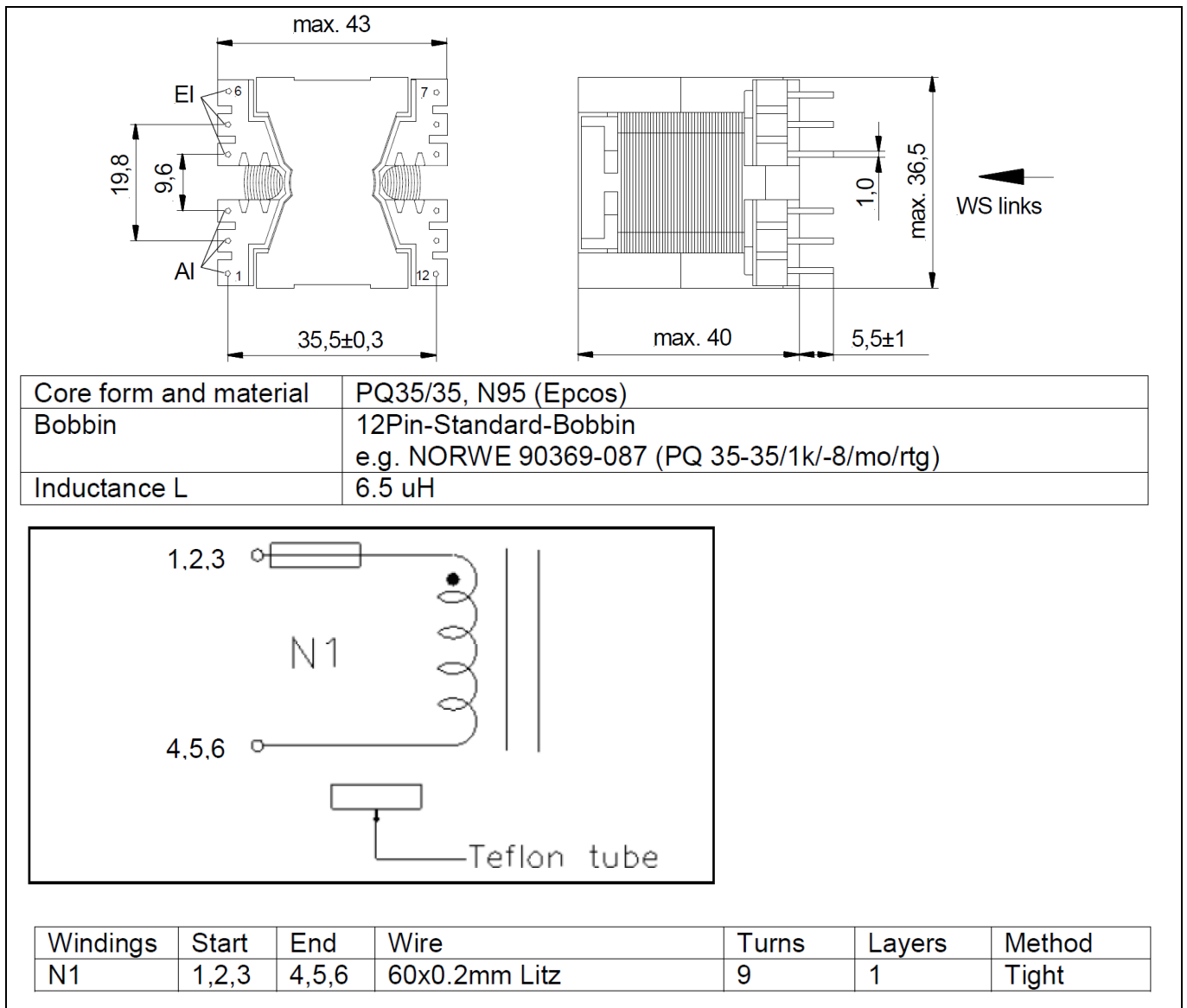
## 3 kW dual-phase LLC demo board

Using 600 V CoolMOS™ CDF7 and digital control by XMC4400



### Board description

#### 3.5.2 LLC resonant choke



The inductor is produced by Infineon's trusted partners in the development and manufacturing of magnetic components:

- [Kaschke Components GmbH](#) – Göttingen, GERMANY
- [ICE Transformers s.r.l.](#) – Loreto Aprutino (Pescara), ITALY

# 3 kW dual-phase LLC demo board

Using 600 V CoolMOS™ CDF7 and digital control by XMC4400



## Board description

### 3.5.3 Auxiliary transformer

PCB

primary / secondary

**Coil build-up:**

primary: Np1: 178 Wdg. CuL D=0,15mm --> Lp=6300uH      D: Durchmesser  
 Np2: 10 Wdg. CuL D=0,25mm

secondary: Ns1: 5 Wdg. CuL D=0,35mm  
 Ns2: 4 Wdg. CuL D=0,35mm

Coresize/Type: E20/10/6 (EF20)  
 Core material: N87 or comparable  
 Airgap: on center tap  
 Coil former: B66206B1110T001 (Epcos)

Operation frequency: 100kHz  
 Isolation class: B (130°C)

Withstand voltage:  
 Np1+Np2 against Ns1+Ns2      2000V / 50Hz / 2s  
 Np1 against Np2                      500V / 50Hz / 2s

			DATE	12.02.2016 15:24			
		Maße in mm	ENGR.	M. Tauer	Flyback Transformer 10W/14V/12V/5V	<b>FinePower GmbH</b> Günzinger Ring 21 33187 Lötterding Tel. +49 (0) 89 20 20 75 9-0 Fax +49 (0) 89 20 20 75 9-22 www.finepower.com	
			APVD.				
REVISION NUM.	DATE	OWNER	STATUS	E01	Saved as	160212_Winding_BIAS_XFMR_V3	Sheet 1/1

The transformer is produced by Infineon’s trusted partners in the development and manufacturing of magnetic components:

- [Kaschke Components GmbH](#) – Göttingen, GERMANY
- [ICE Transformers s.r.l.](#) – Loreto Aprutino (Pescara), ITALY

## 4 Digital control features

The control of the 3 kW dual-phase LLC converter has been implemented using XMC4400, which is part of the XMC™ microcontroller family from Infineon Technologies. This family is based on an ARM® Cortex®-M4 core, and the main features were summarized in section 3.3.5. The following section introduces the main features of the implemented digital control as well as the resources necessary for proper implementation.

### 4.1 Resources and implementation concept

#### 4.1.1 Resources (peripherals)

XMC4400 has been selected due to the complexity of the design, which requires a high number of peripherals as well as a high calculation power. By using the required peripherals for one of the LLC phases as an example, this section presents the necessary resources for the multi-phase LLC design.

Figure 17 depicts the available resources in the selected XMC4400 microcontroller. For a single LLC phase the following resources are used:

- Four timers for PWM generation of both HB and SR switches. XMC4400 includes two different timers (CCU4 and CCU8), which provide not only PWM outputs but a flexible and programmable signal-conditioning scheme thanks to the available interconnections with other peripherals. In the dual LLC, two CCU4 and two CCU8 timers are used for each phase
- Two Event Request Unit (ERU) slices for proper interconnection of the timers. The ERU is a versatile event detection and processing unit which increases the peripheral connectivity
- One high resolution PWM (HRPWM) which includes a high-resolution timer (HRC) and an analog Comparator with Slope Generation (CSG)
- Five ADC channels. These include the input and  $V_{out}$  sensing, which are common for both phases, as well as output current,  $I_{res}$  and temperature, which are measured for each phase
- Apart from compare mode to generate PWM signals, CCU4 timers can be used in capture mode in order to acquire time between different events. Two CCU4 timers are used in capture mode for frequency and time acquisition

Apart from these specific resources, other shared peripherals are required for proper operation of the application:

- One serial communication channel (USIC) is used for communication with the graphical user interface (GUI). The USIC configured in UART mode can be connected to a PC through a serial COM port. This channel is associated with two interrupts for receiving and transmitting the data
- The XMC4400 processor has a 24-bit system timer (SysTick) which counts down to zero from a defined value. This special timer is used in the dual LLC for scheduling purposes to trigger a fixed frequency interrupt. The application SW is executed in this interrupt
- Part of the Flash memory is utilized to store the converter parameters sent via GUI. XMC4400 provides up to 512 kB of Flash memory and therefore, no external EEPROM is necessary

# 3 kW dual-phase LLC demo board

## Using 600 V CoolMOS™ CDF7 and digital control by XMC4400



### Digital control features

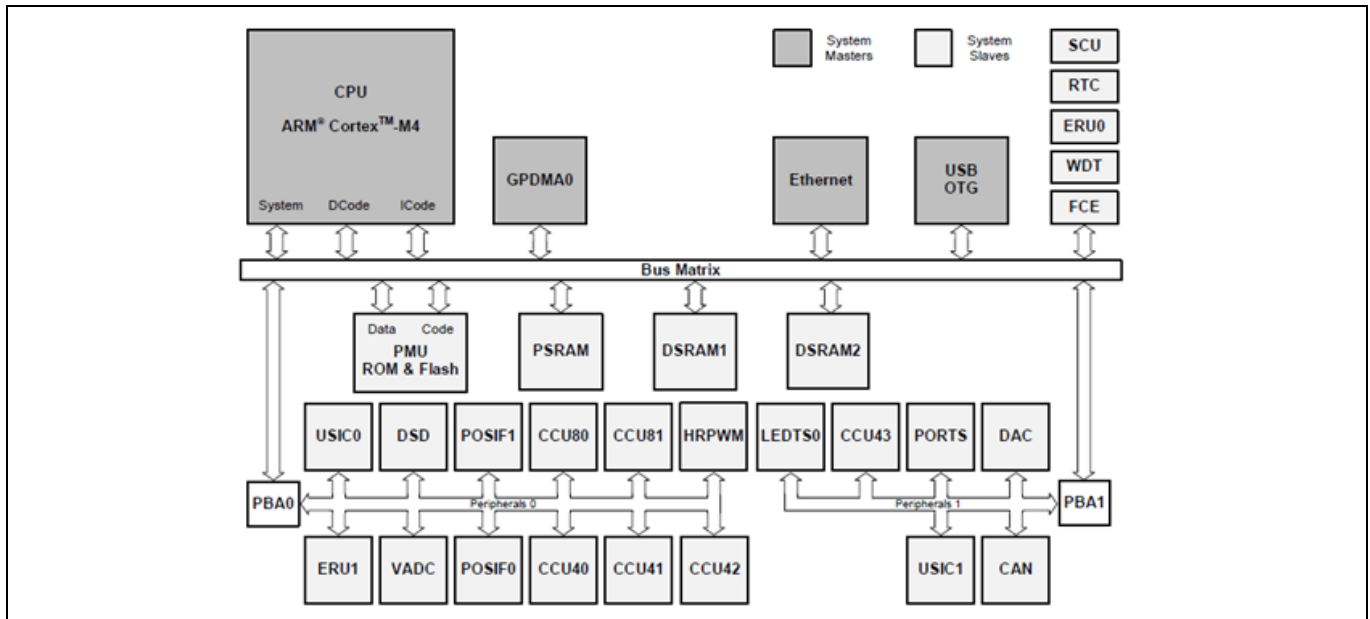


**Figure 19 XMC4400 system resources**

Including the previously mentioned resources, the complete list of resources is summarized in Figure 20.

XMC Peripheral	Resource	used / available
CCU8	timer	6 / 8
CCU4	timer	8 / 16
VADC	channel/pin	8 / 9
USIC	channel	1 / 4
PORTS	pin	33 / 44

**Figure 20 Peripherals used in the dual LLC control implementation in XMC4400**

### 4.1.2 Implementation concept

Besides the previously described peripherals, the implemented control algorithms are executed in a regular time base. The system timer (SysTick) sets this regular time base, thus fixing the sample rate as well as the loop execution. The main functionality of the multi-phase converter is implemented in the control interrupt routine, triggered by the system timer (Figure 21). This functionality includes the following processes:

- Output current limitation protection
- Capacitive mode protection
- Burst mode management
- PI controller
- Start sequence
- Phase shedding
- SR management
- Dead-time calculation
- SW ADC trigger of the control variables

## 3 kW dual-phase LLC demo board

### Using 600 V CoolMOS™ CDF7 and digital control by XMC4400



#### Digital control features

As shown in Figure 18, the PWM signal with a 50 percent duty cycle is generated using a CCU8 timer. The flexibility of this peripheral in the XMC4000 series enables a synchronized trigger of the  $I_{res}$  ADC measurement with the generated PWM signal.

In addition, the versatile ADC enables scheduling of different measurements by using different measurement groups with different triggers and priorities. In the selected implementation, the  $I_{res}$  is measured using the queue function triggered by the PWM. However, the rest of the channels are configured as background measurements with lower priority and are triggered by SW in the control interrupt.

Furthermore, the CCU8 timer can easily be connected to the HR channel of the HRPWM peripheral. This connection not only enables utilization of the 150 ps PWM resolution of this peripheral, but enables the update of the PWM dead time in a safe manner, as will be explained later.

More information about the highly configurable ADC and timer peripherals can be found in [14].

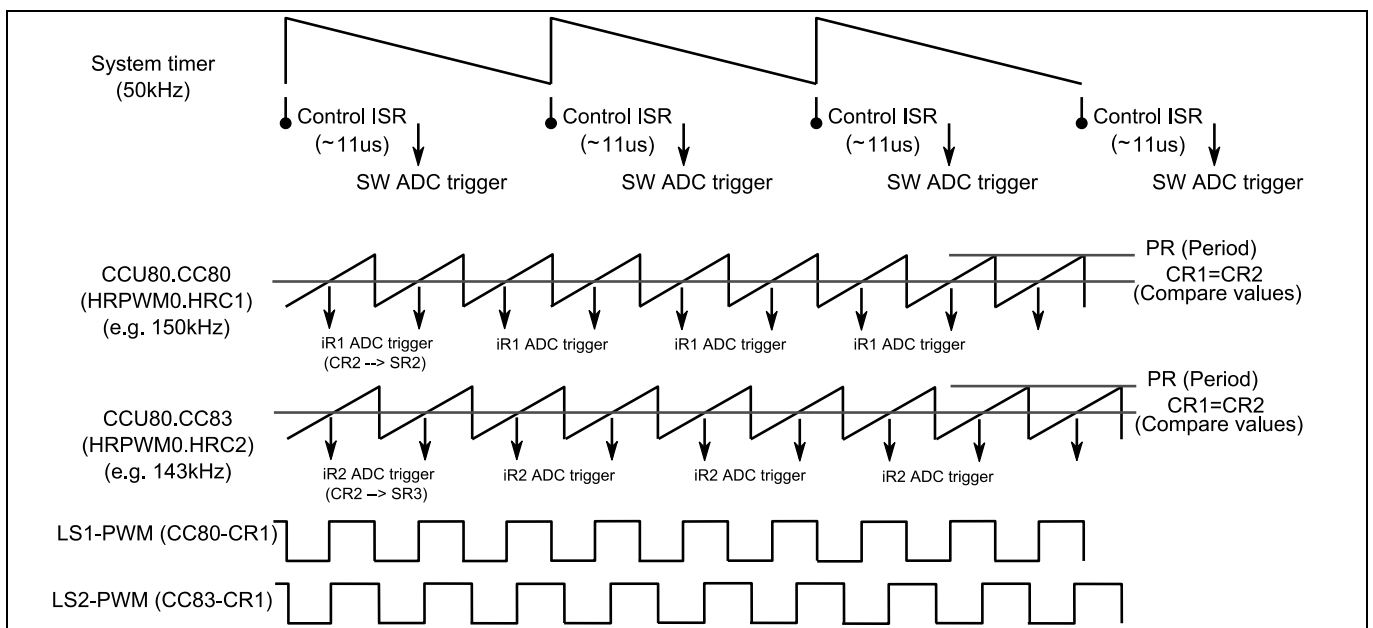


**Figure 21 Time diagram of the 3 kW dual-phase LLC converter digital control implementation**

As shown above, the selected implementation is based on a single interrupt with the highest priority. However, there are other tasks that are implemented in different background processes. Since the interrupt cannot be preempted by the lower-priority tasks, such as the background ones, these last ones are assessed in the remaining processing time between interrupts:

- State machine
- Fault management
- SR time calculation
- Compensator coefficients according to  $C_{oss}$  selection
- Power balance between phases
- Memory observer
- Communication with GUI
- Time counting

In the next sections, the main functionality implemented in the 3 kW dual HB LLC converter will be explained in more detail.

### Digital control features

## 4.2 Current sharing and phase shedding

In section 2.1.2 the concept of implemented current sharing was described. As already explained, both converter phases are controlled using related, but different, switching frequencies in order to balance the current between the phases. This difference in  $F_{sw}$  can be observed in Figure 22 by the difference in phase of both resonant currents at different moments in time, for the same output power. In addition, the number of active phases is modified according to the load level, with the goal of achieving a flat efficiency across a wide load range.

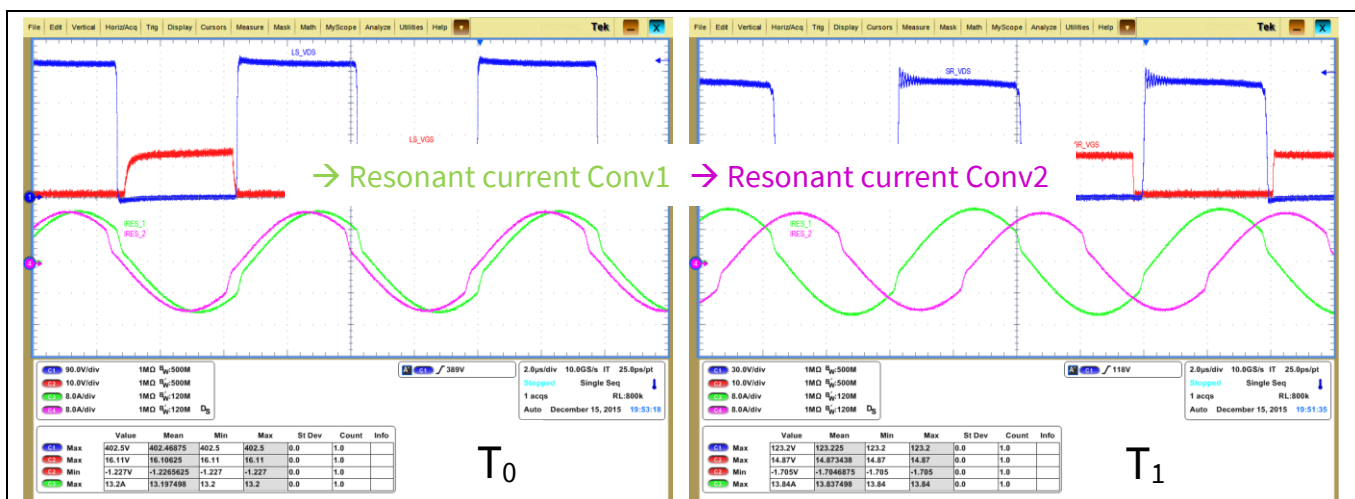


**Figure 22 Phase difference of phase 1 (green) and phase 2 (purple) resonant currents at the same power at two different moments in time**

The implemented current sharing and phase shedding introduced in Figure 8 is redrawn in Figure 23 to show the different blocks involved in the process: both LLC phases (Conv1 and Conv2), a PI controller to ensure  $V_{out}$  regulation, and a current balancer that decides the  $F_{sw}$  to be applied to each phase.

The PI controller is evaluated every control interrupt (50 kHz) according to the sensed  $V_{out}$  and the required voltage target. This voltage target varies during soft-start, and it can have different steady-state values, according to the specifications presented in Section 3.1. The steady-state  $V_{out}$  can be modified via the GUI.

The output of the PI controller, which is the necessary  $F_{sw}$  to match the  $V_{in}/V_{out}$  gain, is fed to a current balancer block, together with the output current measurements of each LLC converter.

### Digital control features

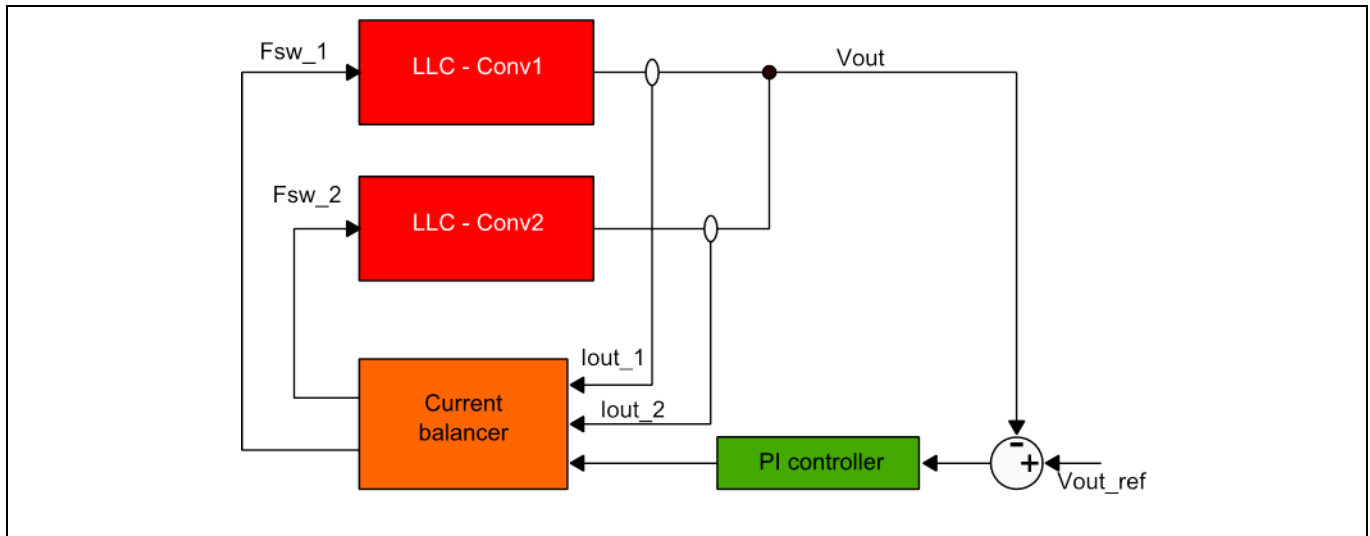


**Figure 23** Block diagram of the current-sharing and phase-shedding functionalities

The current balancer uses this information to calculate the  $F_{sw}$  of both LLC converters, considering not only the  $V_{out}$  regulation but also a maximum current difference of 5 A between the phases. The balance mechanism is based on an intermediate variable, which is modified in an iterative manner, tracking the frequency calculated by the PI controller. The step of the iteration depends on the number of active phases as well as how far the balancer variable is from the output of the PI controller. This mechanism runs as a background process and corresponds to the slow control named as efficiency controller in Figure 8.

The previously presented variable to achieve current balance is slowly modified to guarantee steady-state current sharing and stability. However, a different mechanism is required to handle external perturbations with a fast response. The current balancer variable is therefore immediately modified (in the control service routine running at 50 kHz) when one of the following events is detected: current limitation (Section 4.4.1), load jump and dump, and capacitive mode detection (Section 4.3.2). These three mechanisms are included in the block named as dynamic control in Figure 7.

The efficiency controller, inside the current balancer, is also responsible for the phase-shedding functionality. In this case, the number of active phases is modified to achieve an efficiency curve that is as flat as possible. Two different thresholds separated by a certain hysteresis are defined to decide whether the second phase is enabled or disabled. The current thresholds are defined for the total output current and change according to the  $V_{out}$  target, as shown in Figure 24.

### Digital control features

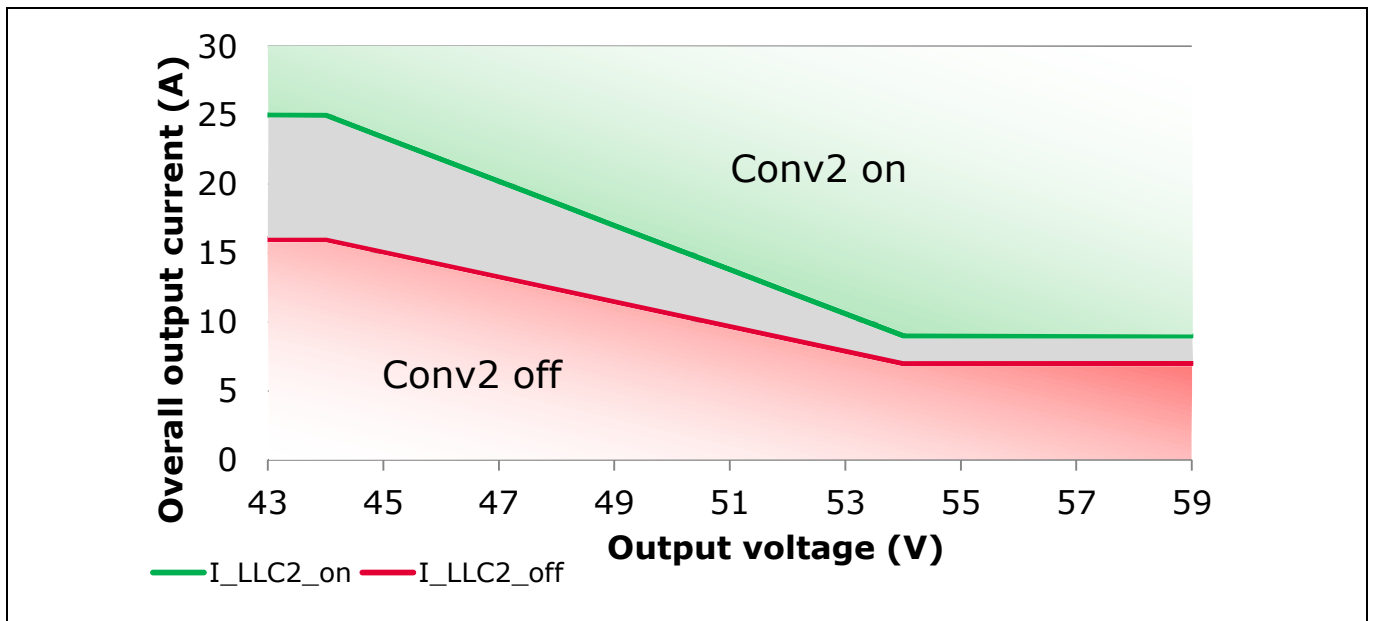


**Figure 24** LLC Conv2 shedding depends on overall output current thresholds for a given target voltage

The presented current levels are applied in steady-state operation of the converter. A third threshold is implemented in order to enable Conv2 as soon as a positive load jump is detected, thus providing an adequate transient response. The enabling of Conv2 for a  $V_{out}$  of 54 V, when a smooth load transition across the defined on-threshold is applied, as shown in Figure 25. As can be seen, the applied load change is small, to change the phase 1  $F_{sw}$ , but enough to start the operation of phase 2, which can be seen in the change of its resonant current.

It must be noted that the second stage operates only in the case that the first phase is active. In case Conv1 is turned off, e.g. in burst mode operation, Conv2 is automatically disabled and later enabled according to the actual current levels.

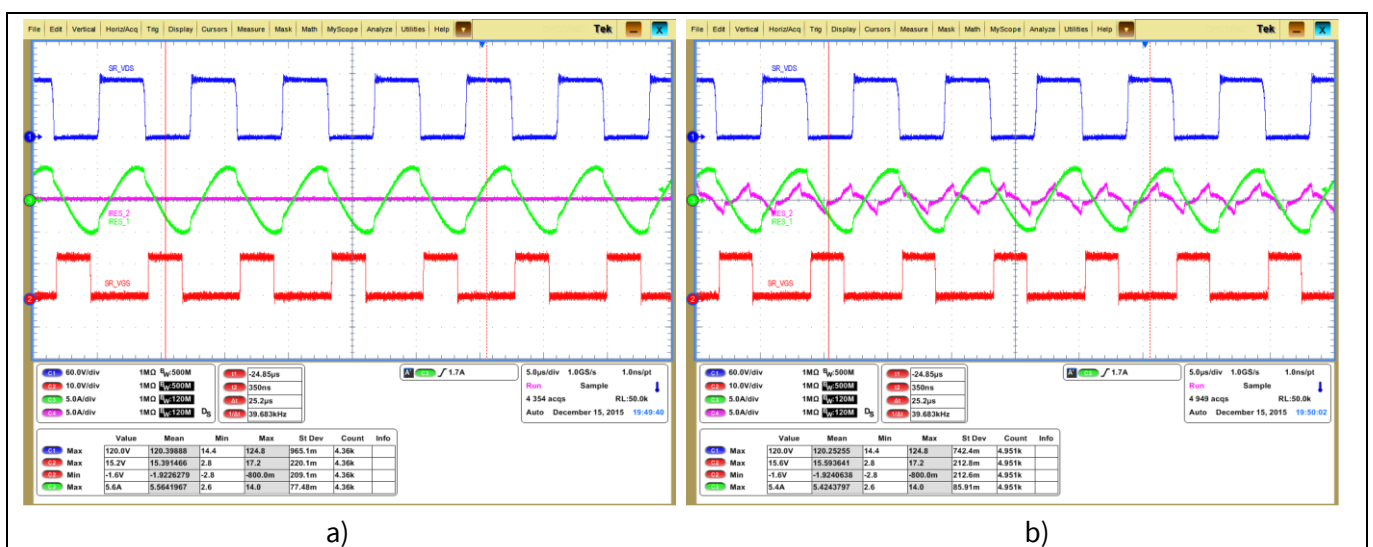


**Figure 25** Resonant current of phase 2 (purple) for single-phase operation (a) and when phase 2 is enabled (b) after the current threshold is reached



## 3 kW dual-phase LLC demo board

### Using 600 V CoolMOS™ CDF7 and digital control by XMC4400

#### Digital control features

- Start-sequence:** With the driver bootstrap capacitor properly charged, the converter operation can be started as shown in Figure 24. In order to avoid hard commutation during the first cycles of the converter start-up, the PWM is driven by the comparison of the  $I_{res}$  with zero. This allows for delaying the change between LS and HS (and vice-versa) after the current zero crossing. As a consequence the change in the current polarity is guaranteed and hard commutation avoided as shown in Figure 25. This phase is applied for 100 us, and the SR switches are kept off



**Figure 28** LS-HS driving signal change is applied with a delay after the  $I_{res}$  crosses zero to guarantee current polarity change and avoid hard commutation

- Soft-start and normal operation:** During the previous phase the time between two consecutive crosses of zero is captured cycle-by-cycle using a CCU4 unit in capture mode. The acquired time is used as the period of another timer, thus generating a timer replica. After the 100 us comparison-driven phase the timer replica is used to drive the PWM, ensuring a smooth transition (Figure 28). At the same moment the  $V_{out}$  is sensed and ramped to achieve the target voltage (soft-start). When the target voltage is achieved (normal operation) SR is managed according to certain conditions, which will be explained elsewhere

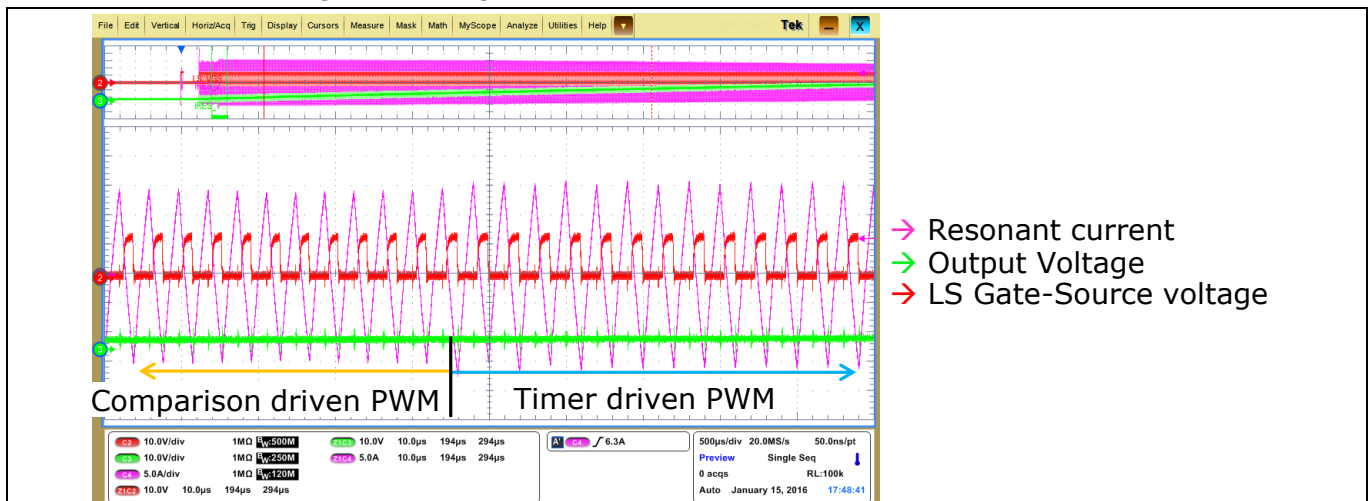


**Figure 29** Smooth transition between comparison-driven and timer-driven PWM operation due to the implemented timer replica

#### 4.3.2 Capacitive mode detection and prevention

In capacitive load mode operation the resonant current leads the voltage in the mid-point of the HB. Therefore, the operation in this mode, or the tendency to move from inductive to capacitive mode, can be monitored by knowing the phase difference between the previously mentioned current and voltage.

In the design shown here, for each converter, this phase information is obtained by capturing the time between the PWM output edge and the corresponding zero crossing detection of the resonant current (Figure 30). In order to increase the robustness of the implementation, the previous PWM edge to the selected zero crossing is used for the time captured, as shown in Figure 27. This modification enables measurement of the negative phase for fast capacitive mode detection. With the captured time information, the actual phase difference can be calculated by SW, since the switching period is known.

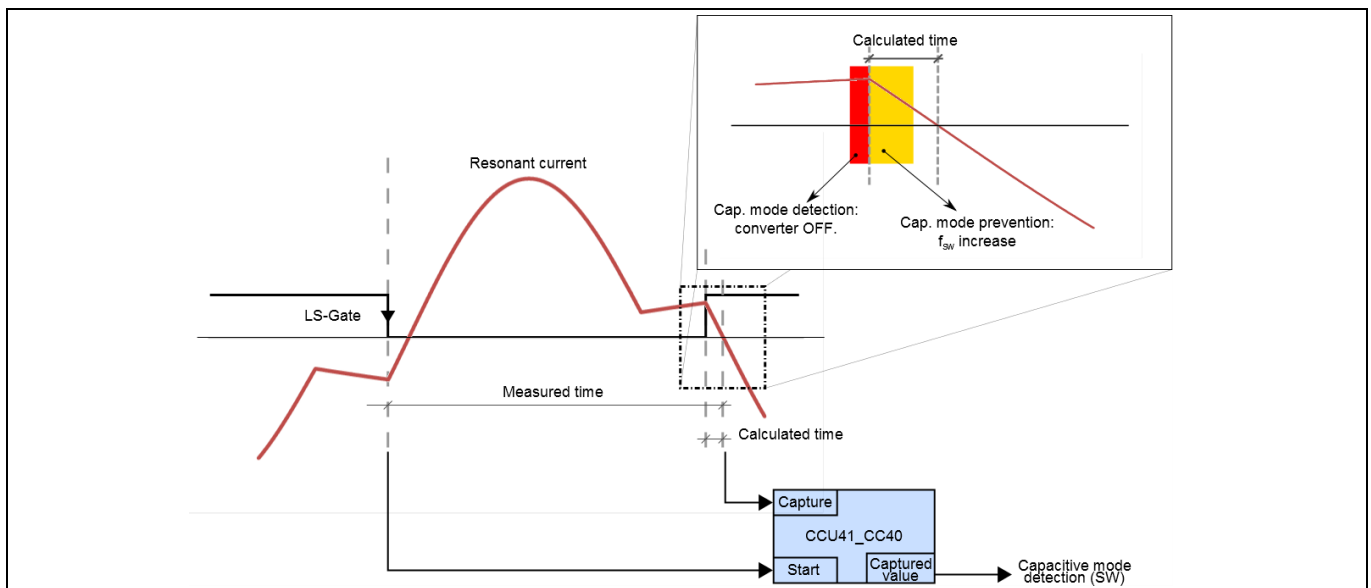


**Figure 30** CCU4 timer in capture mode to acquire the phase difference between voltage and current and capacitive mode prevention and detection phase thresholds

With this phase difference information two different protection mechanisms can be triggered: capacitive mode prevention and capacitive mode detection.

- When the captured phase difference decreases toward zero under a certain defined threshold, the prevention algorithm is activated. This prevention consists of increasing the  $F_{sw}$  by decreasing the  $V_{out}$  target. The implemented algorithm can shut down the converter if, after several successive tries at increasing the  $F_{sw}$ , the phase difference remains under the defined threshold
- The second mechanism is capacitive mode detection. Capacitive mode is detected if the captured threshold is zero or negative for two consecutive sampling periods. As a result of detecting capacitive mode the converter is immediately turned off. The latching behavior of the protections can be selected via the GUI, as explained later in this document

#### 4.4 Protections

Two different levels of protections have been implemented in the microcontroller, depending on the variable being monitored. Those that require fast reaction (linked to the input and output current) are evaluated in the interrupt service routine associated to the control loop. The other variables are monitored in the background process with different filter times, as explained below.

#### Digital control features

The latching behavior of the implemented protections can be controlled using the GUI, with the exception of the overtemperature protection, which is always the latching type. By default the protections are configured to be non-latching, and the converter will try to restart 2 s after the fault has been detected.

#### 4.4.1 Overcurrent protection

Different limits and algorithms have been implemented for each phase of the dual LLC converter regarding output current (Figure 31). A first limit is set to distinguish between normal operation and overcurrent conditions. If the sensed output current is over this threshold, either current limitation or Over Current Protection (OCP) mechanisms are applied.

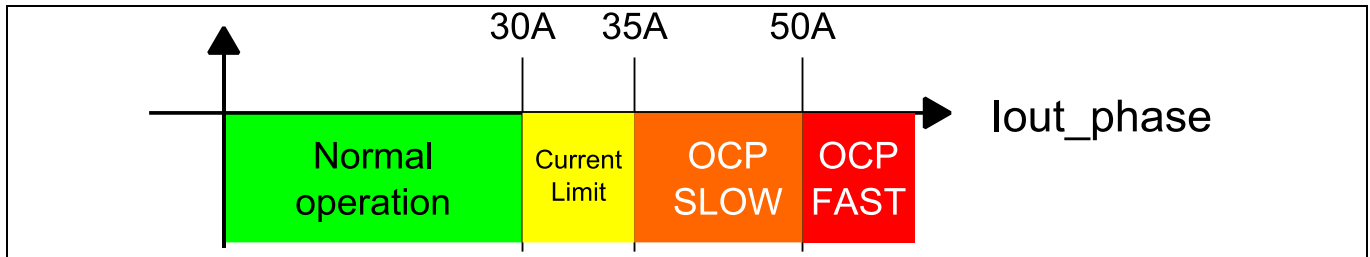


**Figure 31** Output current monitoring limits

For the fastest current protection, OCP FAST in Figure 31, the sensed current is compared with the highest of the defined thresholds (50 A). The comparison is assessed every interrupt cycle (20  $\mu$ s) and it is active after the soft-start phase of the starting sequence is completed.

A second level of OCP is defined with an intermediate threshold (35 A). In this case the protection is triggered if the sensed current remains over this value (OCP SLOW in Figure 31) during 40 ms.

If the sensed current is not reaching the OCP levels but is over the normal operation range, the current limit mechanism is triggered (Figure 32). The current limitation is applied via the  $V_{out}$  target reduction, thus limiting the  $F_{sw}$ . Different scenarios are possible in this situation depending on the number of active phases:

- If only phase 1 is enabled, the current limitation is obviously applied based on the output current of that phase
- In case both phases are enabled, the  $V_{out}$  target reduction is applied considering only the output current of phase 2
- Furthermore, if both phases are active and current over the 30 A threshold is detected in phase 1, the current balance is modified to increase the current provided by phase 2

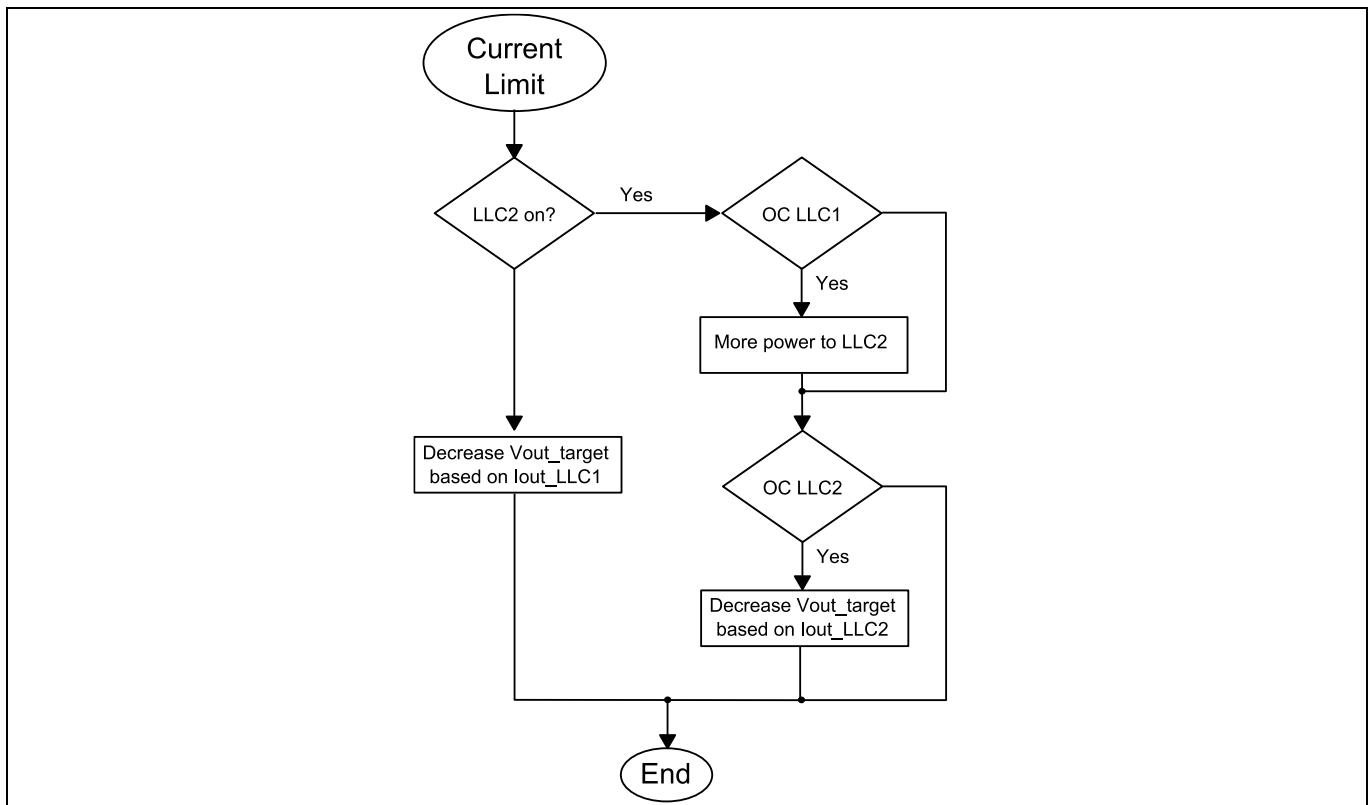


**Figure 32** Flow diagram of the current limit algorithm

For any of the previously described current limitation scenarios, a fault is triggered if the current remains over the lowest threshold (30 A) during 2 s.

Besides the output current protections mentioned, there is an input OCP based on the  $I_{res}$  measurement. Unlike the other sensed variables in the system, the  $I_{res}$  ADC measurement is synchronized with the PWM of each phase (Figure 21). Therefore, accurate information of the  $I_{res}$  value of each phase is obtained. This information is used to detect either overcurrent or capacitive mode operation, by means of a comparison with a fixed current threshold.

#### 4.4.2 Input and output voltage monitoring

Both  $V_{in}$  and  $V_{out}$  are constantly monitored during operation of the dual LLC. In the case of the  $V_{out}$ , a fault is set when the sensed and filtered value is above a defined level. This limit can be configured using the GUI and is set to 62 V by default. Setting the fault implies that the converter turns off. The resumption of operation depends on the selected latching behavior in the user interface, as explained previously.

Regarding the  $V_{in}$ , both the upper and lower limits are defined. If the filtered sensed  $V_{in}$  is outside the defined range the converter remains off. However, the converter is not latched and the operation resumes when the  $V_{in}$  is inside the range. The minimum and maximum limits for this protection are fixed to 345 V and 415 V respectively, and cannot be modified via the user interface.

#### 4.4.3 Other protections

Apart from the current and voltage protections for both input and output variables, other protections have been implemented in the presented converter.

### Digital control features

Using the  $V_{out}$  and output current measurements, the output power of each converter can be calculated. If the total output power is higher than a defined threshold, a fault is triggered and the converter is turned off. The limit cannot be modified and it is set by default to 3.2 kW. The same fault is reported in the user interface if the current limitation algorithm is not able to reduce the output current after 2 s.

An open-loop operation protection has also been implemented in the dual LLC converter. In open-loop operation, the  $V_{out}$  FB is lost and the controller will try to increase the  $V_{out}$  by reducing the  $F_{sw}$ . Therefore, this condition is detected if both phases are operating at a minimum frequency for 1 ms, triggering the corresponding fault.

The last of the protection implemented is temperature protection for each phase of the converter. The temperature of each phase is sensed using NTCs coupled to the main transformer, and this information is fed to the microcontroller. According to the sensed temperature the fan is turned on (over 45°C) and off (under 35°C). Furthermore, a protection is triggered if the sensed temperature is over 80°C. This protection is always the latching type, and it cannot be modified using the GUI, thus a power reset of the converter is required.

## 4.5 Burst mode and SR management

In very light load or no-load conditions, burst mode is a common choice to maintain ZVS operation and solve regulation problems [8]. In the implementation shown, burst mode operation is triggered according to the  $V_{out}$  level and the frequency of operation. An OV of 750 mV will start burst mode operation if the converter is operating at maximum frequency. Furthermore, if a 2.5 V OV is detected, regardless of the  $F_{sw}$ , the converter is turned off and burst mode operation is started. The following table summarizes the conditions that trigger burst mode operation.

Overvoltage	Switching frequency	Burst mode
> 750mV	max. freq.	YES
	< max. freq.	NO
> 2.5V	Not considered	YES

**Figure 33 Burst mode trigger conditions in the 3 kW dual LLC converter**

Figure 32 (left) shows the primary-side waveforms of Conv1 during burst mode operation. It must be noted that burst mode operation is triggered in light-load operation and only Conv1 is enabled. The converter operation is resumed during burst mode when the  $V_{out}$  target is reached again. In this condition, the starting sequence presented in section 4.3.1 is implemented to avoid hard-commutation, as shown in Figure 32 (right).

# 3 kW dual-phase LLC demo board

Using 600 V CoolMOS™ CDF7 and digital control by XMC4400



## Digital control features

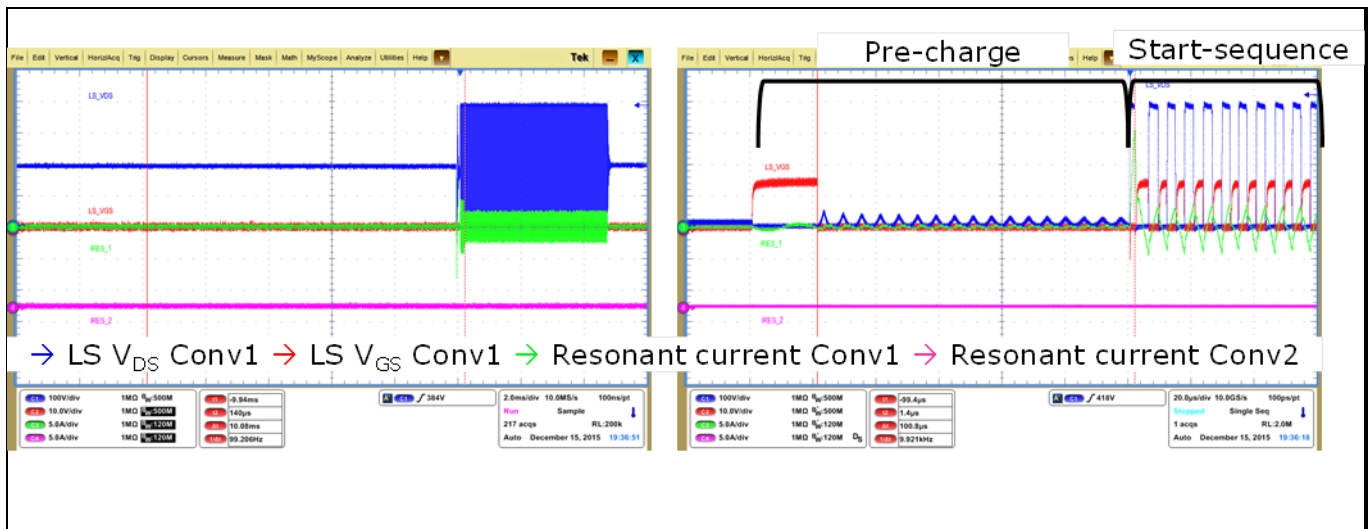


**Figure 34** Burst mode operation of the dual-phase LLC converter (left) and detail of the starting sequence during burst mode (right)

SR management is applied to both phases independently. If burst mode operation is triggered, the synchronous rectifiers (SR) are turned off to avoid reverse power flow and possible capacitive mode operation. Furthermore, SR switches are turned off for the same reason if a load jump is detected, as mentioned in Section 2.2. These conditions together with steady-state operating conditions to disable the SR switches are summarized in the following tables.

OFF conditions	
OR	Iout_phase < 4A
	I resonant > 9.25A
	Vout < 42V
	Load change > 8A
Burst mode	

**Figure 35** Synchronous rectifiers off conditions

Previously the off conditions were presented. On the other hand, SR switches for each phase are allowed to be turned according to the conditions present. When SR is enabled a soft-start of the on-time is applied to enable a smooth gain transition in the converter operation.

SR ON conditions	
AND	Iout_phase > 4.5A
	I resonant < 9A
	Vout > 43V
	Load change < 8A

**Figure 36** Synchronous rectifier on conditions

## 3 kW dual-phase LLC demo board

### Using 600 V CoolMOS™ CDF7 and digital control by XMC4400

#### Digital control features

#### 4.6 Adaptive dead time

In order to maintain proper ZVS operation for different load and line conditions, a variable dead time between the driving signals of the HB is necessary. For a given design ( $L_m$ ) and a given switch (time-related  $C_{oss}$ ) the necessary dead time for a specific operation frequency can be calculated based on the following equation:

$$t_{DT}[ns] = DT\_offset + 2 \cdot \sqrt{2} \cdot \pi^2 \cdot C_{oss} \cdot L_m \cdot f_{sw}$$

This equation is implemented in the dual HB LLC SW. Therefore, the proper dead time for the operating  $F_{sw}$  of each phase is calculated. This calculation is done every control interrupt cycle (20  $\mu s$ ), according to the new calculated  $F_{sw}$ .

The required parameters can be provided through the GUI. Figure 37 shows the window of the GUI where the necessary parameters for the dead-time calculation can be provided. As an example of the required capacitance value, the time-related  $C_{oss}$  of two CoolMOS™ transistors extracted from the available online datasheet are presented. If different CoolMOS™ transistors from different generations are used, it might be necessary to adjust the dead time. Therefore, a variable offset can be modified using the GUI for more precise adjustment.

The HRPWM peripheral included in the XMC™ enables safe modification of the dead time during operation. This safe update is possible due to the shadow transfer mechanism for the dead time included in the HRC of the HRPWM [14].



IPW60R031CFD7:	Effective output capacitance, time related <sup>3)</sup>	C <sub>o(tr)</sub>	-	2101	-	pF	I <sub>D</sub> =constant, V <sub>GS</sub> =0V, V <sub>DS</sub> =0...400V
----------------	--	--------------------	---	------	---	----	--

**Figure 37 GUI window to provide the necessary parameters for adaptive dead-time calculation for IPW60R031CFD7 CoolMOS™ transistor extracted from the datasheet**

#### 4.7 Loop compensation parameters

As mentioned in Section 2.3, the total amount of output capacitance in the PSU is affected by the total capacitance present outside the unit. The total amount of capacitance seen by the PSU influences the loop stability and, therefore, the response of the unit to load and line jumps as well as any other external perturbation. Through the user interface developed for this dual-phase LLC converter, three different capacitors can be selected according to the output capacitor mounted by the user.

The three selectable capacitor values (4 mF, 6 mF, and 8 mF) correspond to three sets of integral and proportional gains for the implemented PI controller in the voltage loop. The adequate set of integral and proportional gains is selected before the converter starts in accordance with the selected output capacitor in the user interface.

### Digital control features

#### 4.8 Graphical User Interface (GUI)

The GUI is a key part of our design concept, with the goal of enabling engineer interaction with the 3 kW dual-phase LLC during its evaluation on the bench. The main features of it were outlined in Section 2.3.

The physical aspects of the GUI are shown below – four main blocks can be seen:

- Setting and control: set the desired values for electrical parameters, converter operation and protections
- Measured values: measure the most relevant voltages, currents, and temperatures
- Status register: short description of the converter operating conditions
- Fault register: flags showing the type of detected malfunction in case of forced shut-down

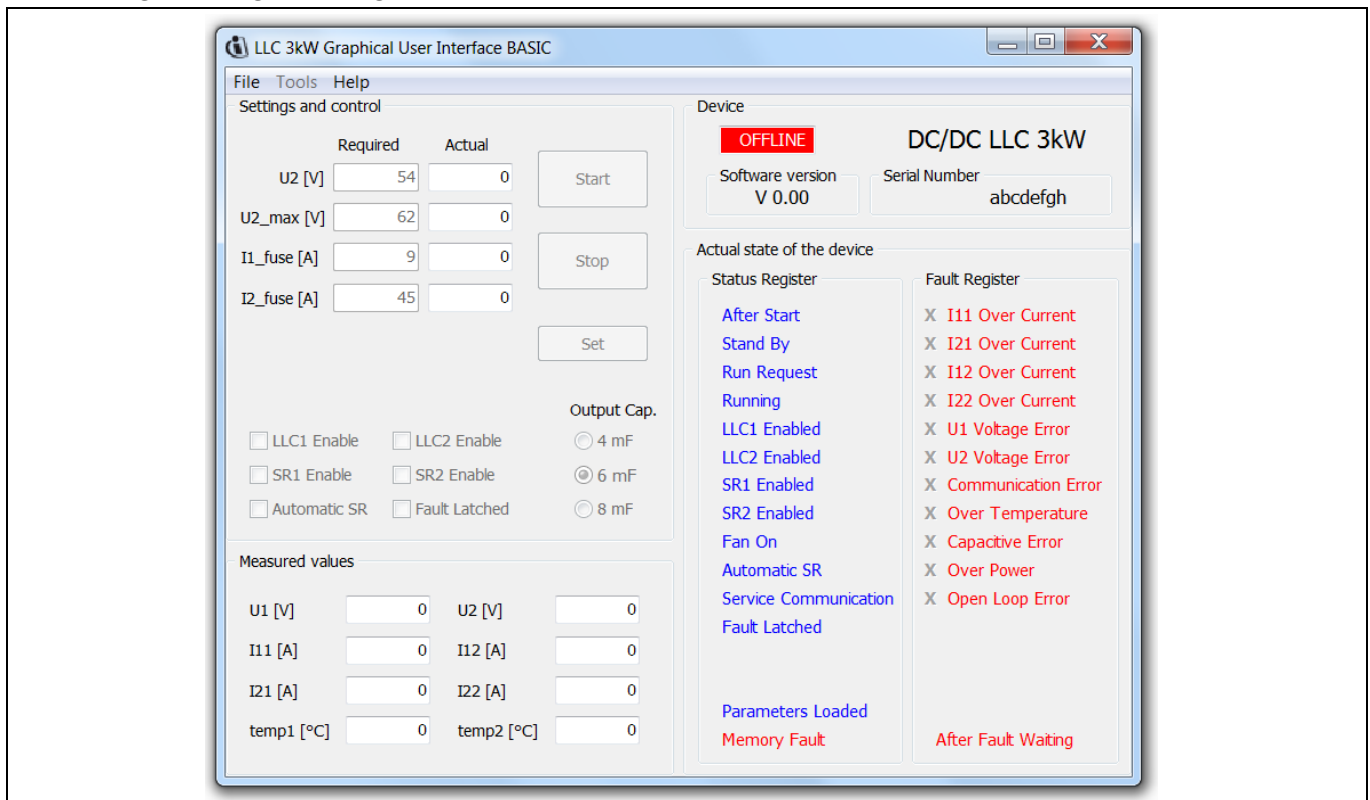


Figure 38 LLC 3 kW Graphical User Interface (GUI)

The benefits are evident: the GUI is an intuitive and user-friendly tool, even enabling changing the mode of operation of the converter without the need to modify any lines of code. It also provides real-time information on the status of the board, assuring constant monitoring, including in the case of shut-down due to the triggering of various protections.

By clicking on the icon below, the reader can find a detailed step-by-step guide to getting started with the GUI.

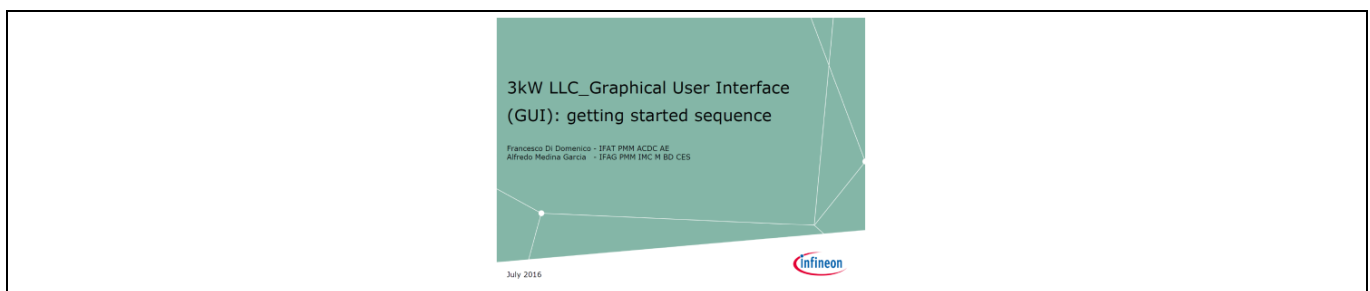


Figure 39 3 kW LLC GUI – getting started

# 3 kW dual-phase LLC demo board

Using 600 V CoolMOS™ CDF7 and digital control by XMC4400

## Performance evaluation

### 5 Performance evaluation

This section provides an overview of the general operation and performance of the 3 kW dual-phase LLC.

The results were achieved on the primary side of both phases of the 600 V CoolMOS™ CFD7 in the TO-247 package (IPW60R031CFD7).

#### 5.1 Waveforms captured in significant operation modes

The following figures show some of the most significant operation modes of the 3 kW dual-phase LLC.

Figures 36–38 illustrate the shape of the primary resonant tank and the gate and drain voltages measured on the low side (LS) MOSFET of Conv1. The unsynchronized switching frequencies of the two converters can be easily seen from the resonant current waveforms. The reduced peaks on the  $V_{DS}$  and  $V_{GS}$  demonstrate the accurate Infineon driving scheme and layout, which get the best performance out of the latest 600 V CoolMOS™ CFD7 technology. Special care must be taken in the selection of the gate resistances located in the turn-on and turn-off path of the HB MOSFETs: the choice is normally a trade-off between the efficiency target (especially related to switching losses) and reliability topics (mostly related to drain-source voltage de-rating guidelines). In our case, the selection of  $R_{G,on} = 47 \Omega$  and  $R_{G,off} = 1 \Omega$  enabled us to combine excellent ZVS behavior and reduced switching losses with very limited stress on the device. Bear in mind that the value of these resistances must be selected case by case, according to the PCB layout, the control applied during the start-up sequence, or output short-circuit protection for example.

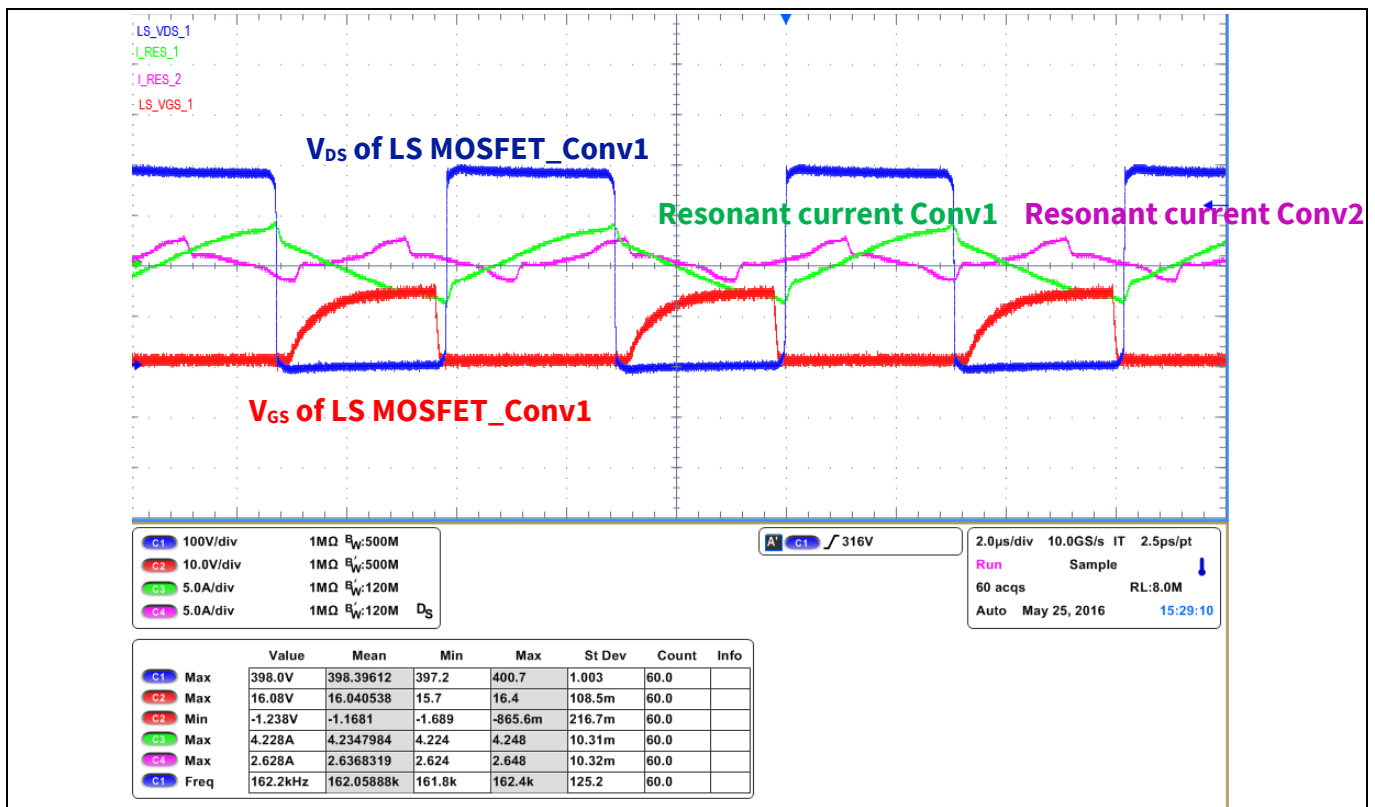


Figure 40 Resonant currents:  $V_{GS}$  and  $V_{DS}$  on the LS MOSFET (Conv1) at 10 percent load

# 3 kW dual-phase LLC demo board

Using 600 V CoolMOS™ CDF7 and digital control by XMC4400



## Performance evaluation

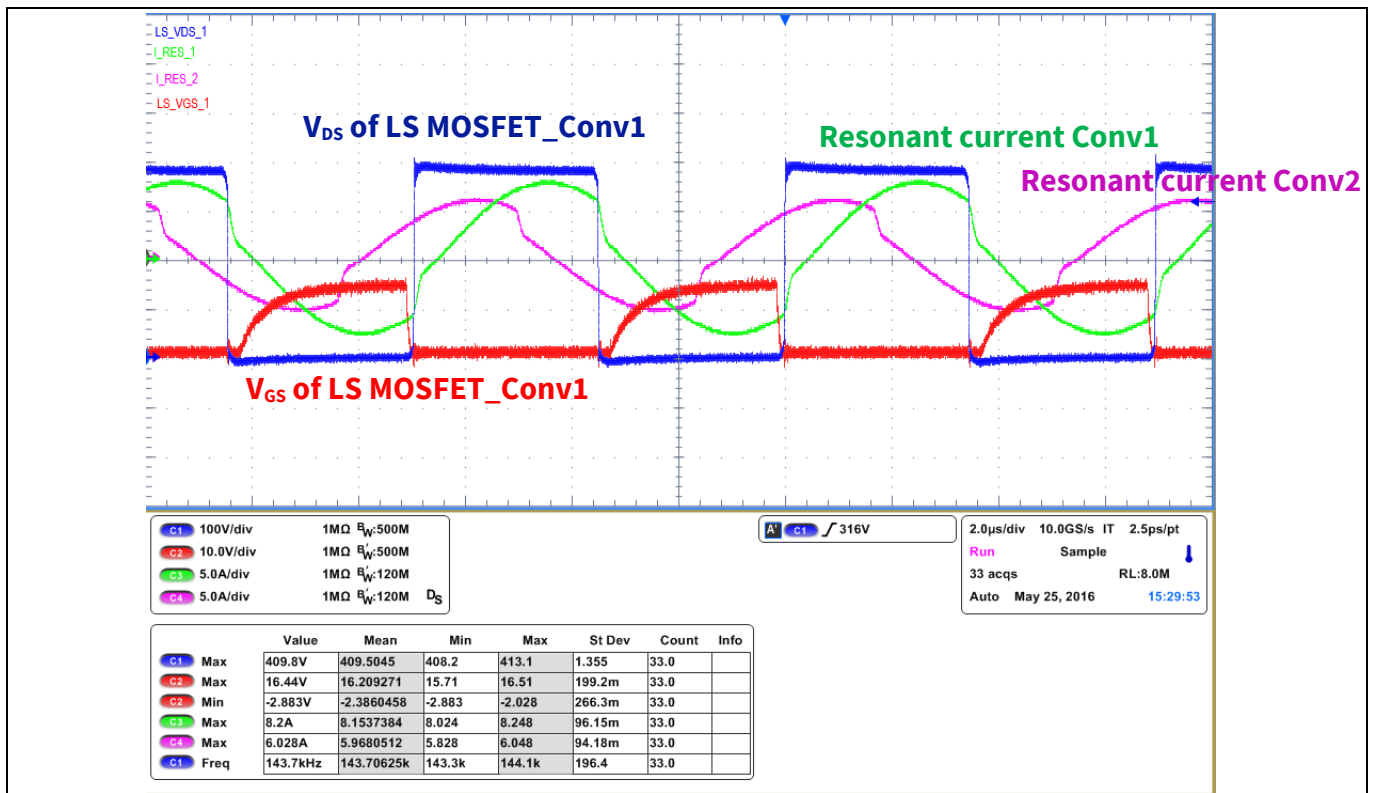


Figure 41 Resonant currents: V<sub>GS</sub> and V<sub>DS</sub> on the LS MOSFET (Conv1) at 50% load

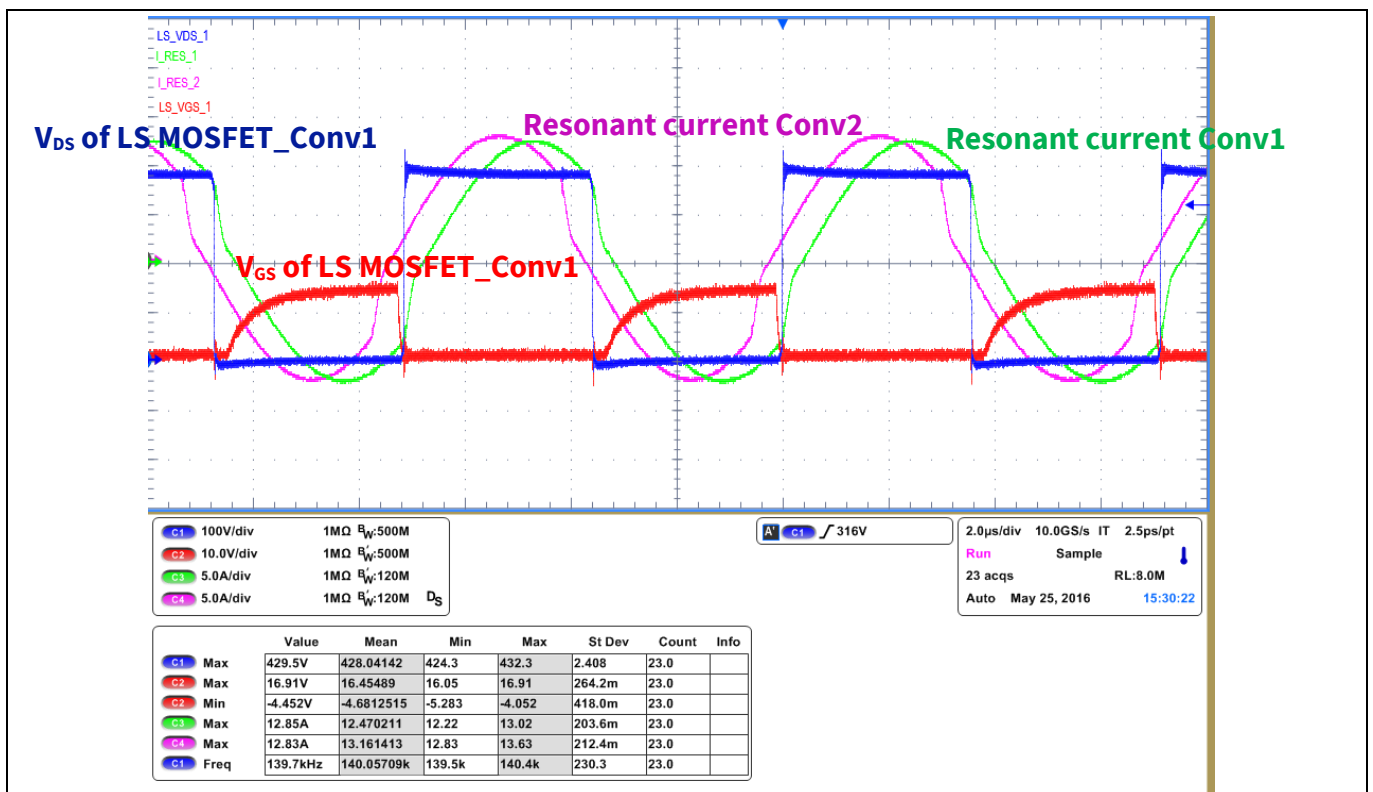


Figure 42 Resonant currents: V<sub>GS</sub> and V<sub>DS</sub> on the LS MOSFET (Conv1) at 100 percent load

Figures 39–40 focus on the ZVS behavior, which is achieved even at very light load.

# 3 kW dual-phase LLC demo board

## Using 600 V CoolMOS™ CDF7 and digital control by XMC4400



### Performance evaluation

You can easily see the achievement of ZVS from the absence of the Miller Plateau in the  $V_{GS}$  waveforms, which is a sign that the  $V_{DS}$  returns to zero before the device is turned on. This will obviously minimize the device switching losses, which will only affect the turn-off transition, thus maximizing the converter's efficiency, especially at light load, where the switching losses are dominant.

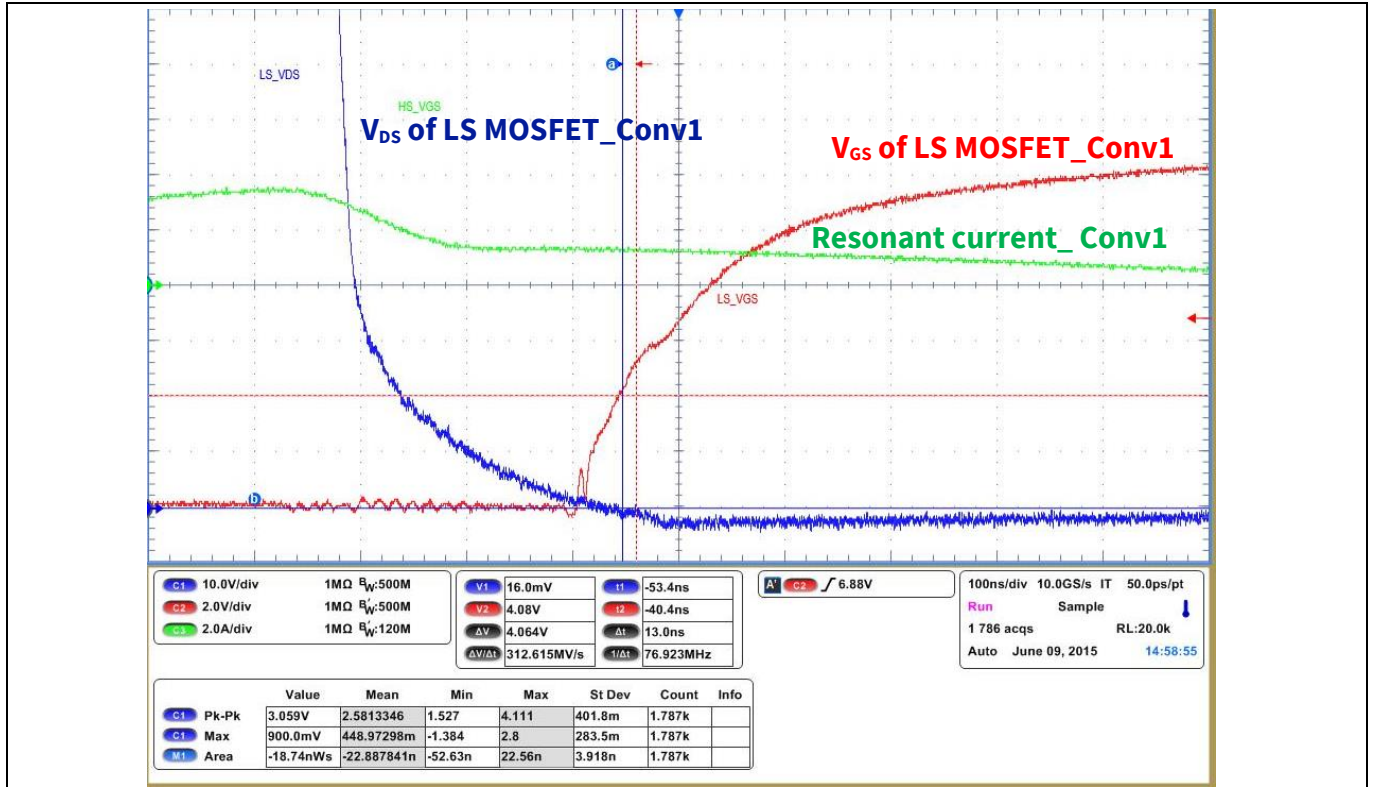


Figure 43 Full ZVS turn-on at only 3 percent load (90 W) and  $V_{in} = 380$  V DC (Conv1)

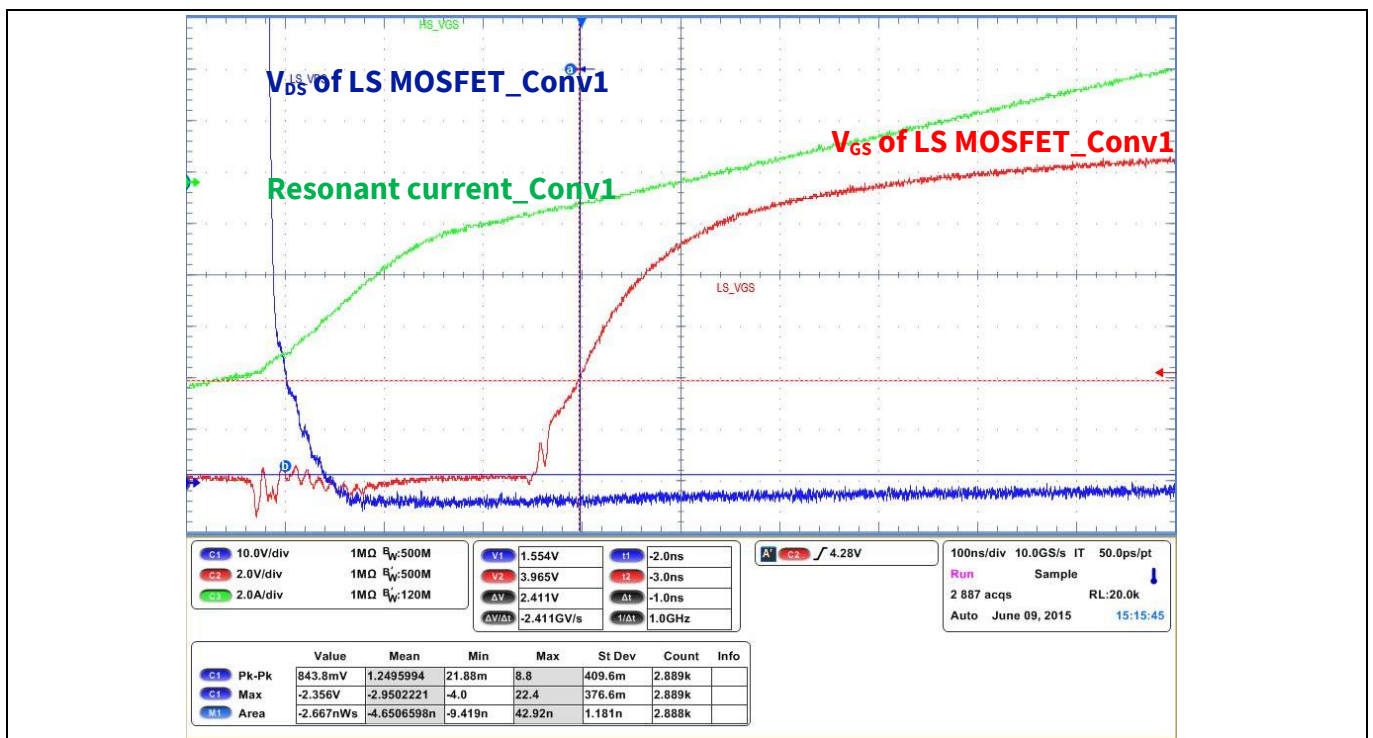


Figure 44 Full ZVS turn-on at full load (3000 W) and  $V_{in} = 380$  V DC (Conv1)

### 3 kW dual-phase LLC demo board

Using 600 V CoolMOS™ CDF7 and digital control by XMC4400

#### Performance evaluation

Figures 41–42 show SR operation at 10 percent and 100 percent load: the  $V_{DS}$  reduced peak measured on the SR MOSFET is the result of an accurate layout and transformer construction, but is also linked to the very low  $Q_{rr}$  offered by the OptiMOS™ 5 technology.

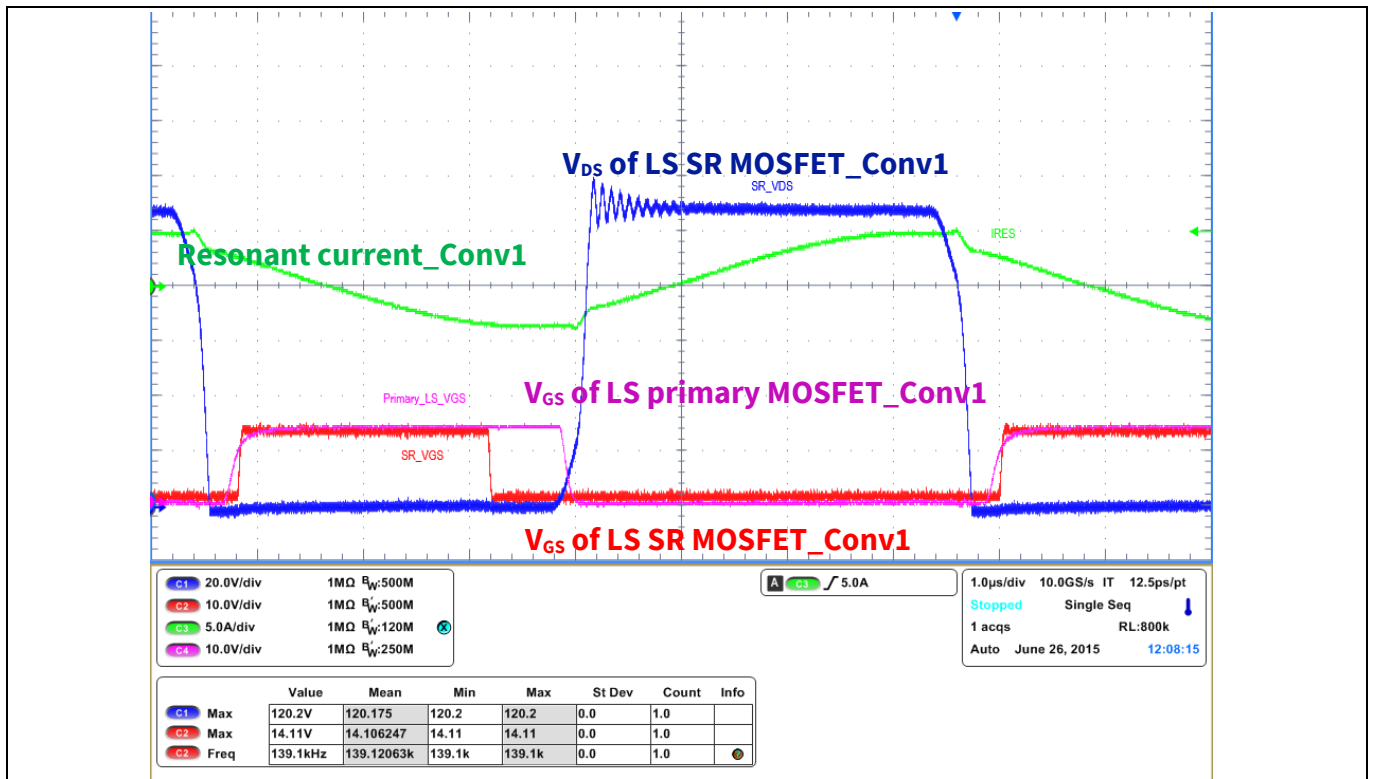


Figure 45 SR MOSFET operation at 10 percent load and  $V_{in} = 380 V_{DC}$  (Conv1)

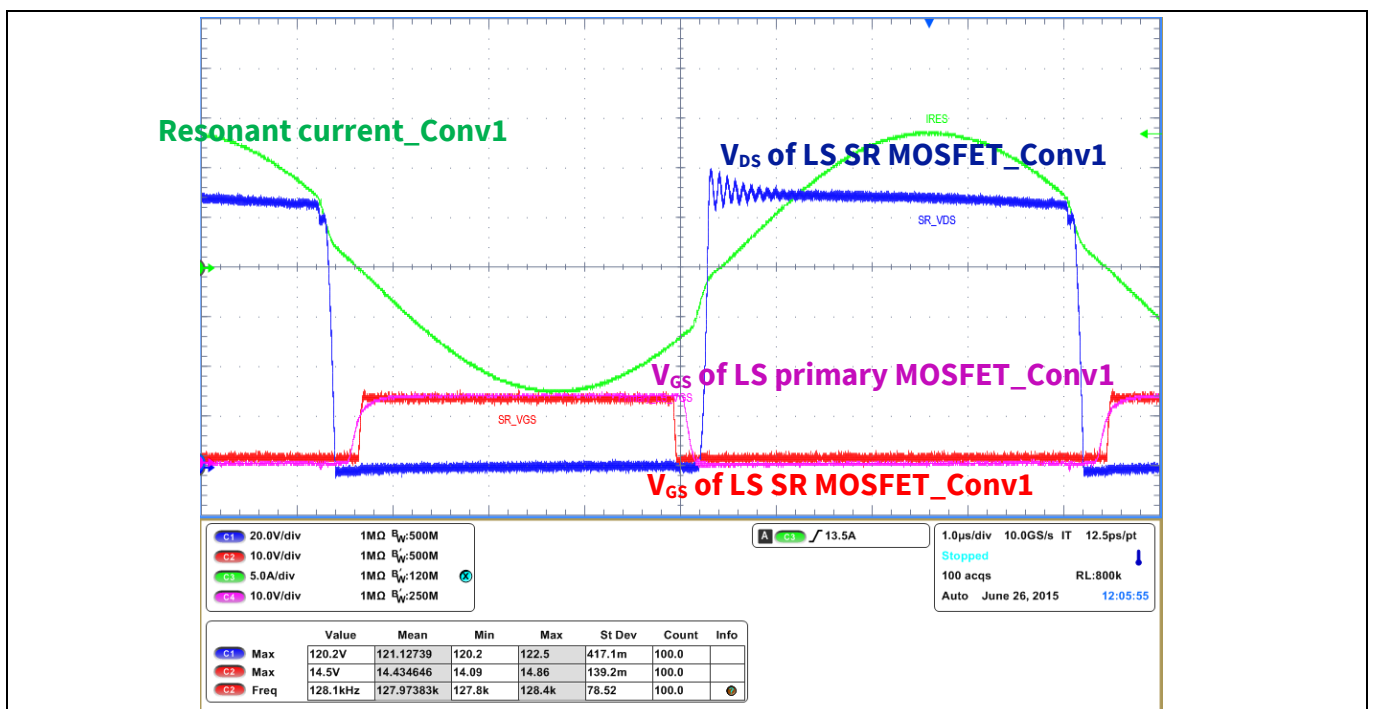


Figure 46 SR MOSFET operation at full load and  $V_{in} = 380 V_{DC}$  (Conv1)

### Performance evaluation

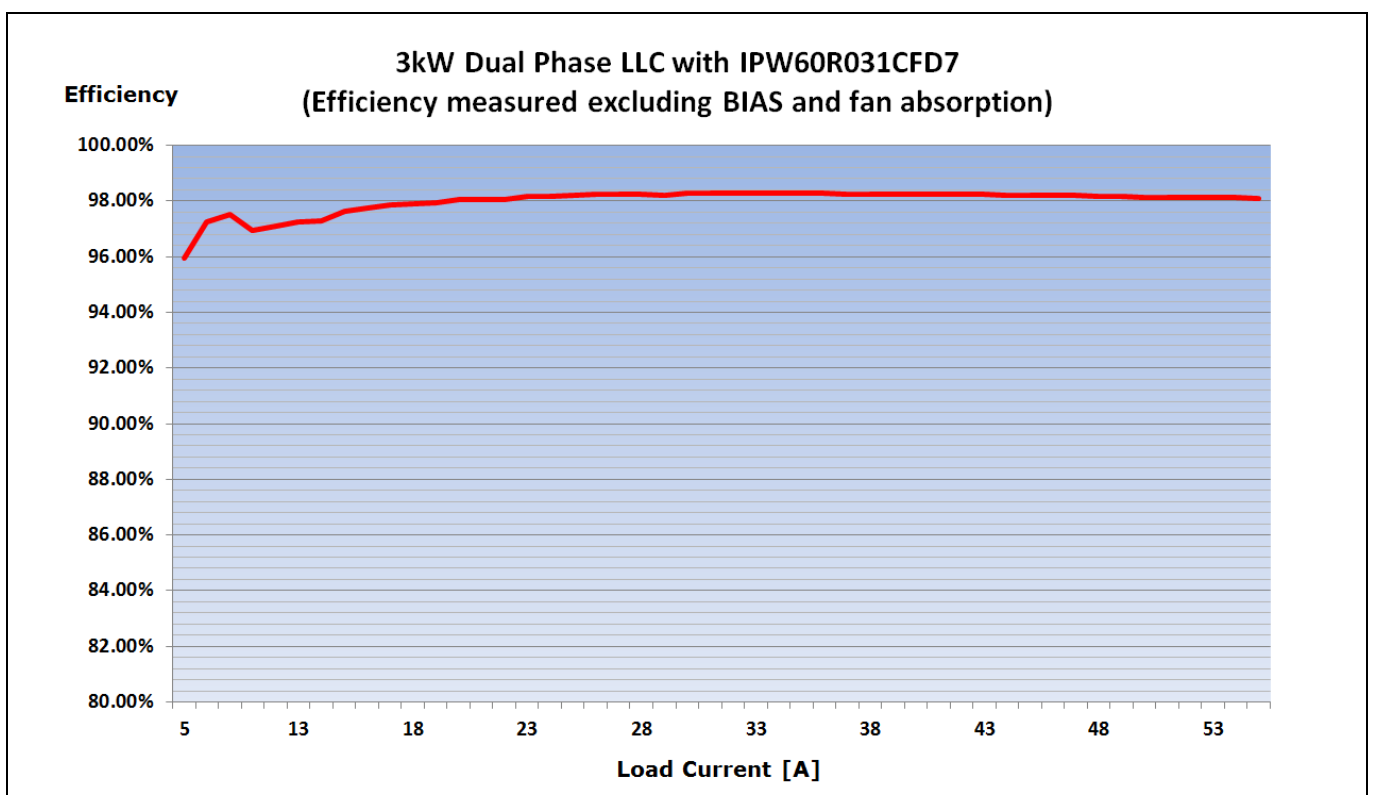
## 5.2 Efficiency plot

Figure 43 reports the efficiency plot measured on the 3 kW dual-phase LLC assembled with IPW60R031CFD7. The fans and BIAS consumption are not included in the measurements shown.

All measurements have been performed in a fully automated setup and according to the methods described in [13].

A very flat plot can be observed: this is the well-known effect of the phase shedding. Moreover, the efficiency at 100 percent is not much lower than the 50 percent load, which gives significant benefits from the thermal perspective.

For the sake of completeness, it should be stated that including BIAS and fan consumption would generate around 3 W additional losses, which would reduce the efficiency by 1 percent at 10 percent load, but only 0.1 percent at full load.



**Figure 47 Efficiency versus load measured with IPW60R031CFD7 at  $V_{in} = 380$  V DC**

The plot above shows that the performance targets set in the technical specification at the beginning have been completely fulfilled.

To highlight the crucial contribution of the 600 V CoolMOS™ CFD7 MOSFET usage in the two HB LLCs, it is worth showing another graph in Figure 44 that includes the  $\Delta\eta$  measured in the same board in comparison with three competitors' fast body diode devices in a comparable  $R_{DS(on)}$  range.

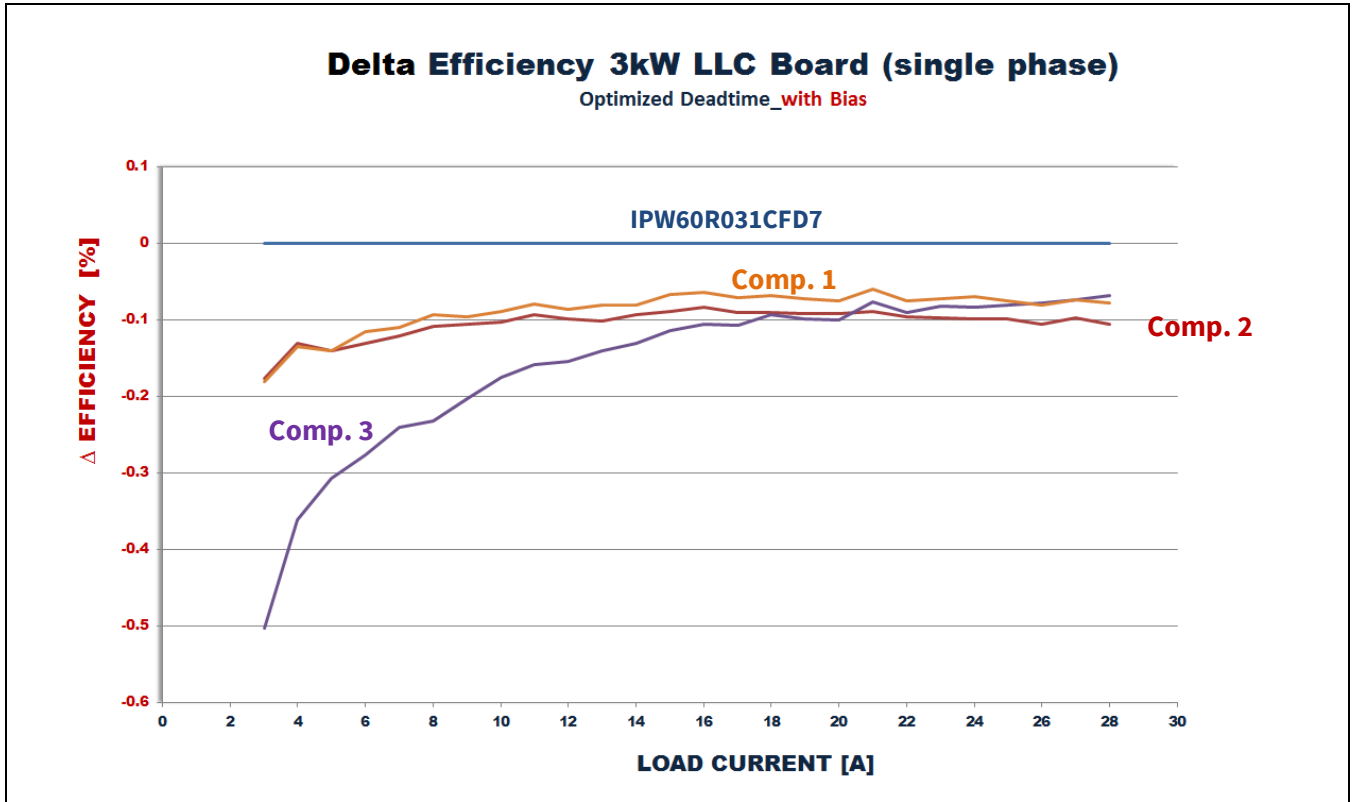


**Figure 48 IPW60R031CFD7 vs three competitors in 3 kW dual-phase LLC**

The plots have been acquired during operation with only one phase activated (1500 W), in order to increase the measurement accuracy, especially at very light load operation. IPW60R031CFD7 is able to achieve better efficiency compared to the three competitors with similar  $R_{DS(on)}$  across the entire load range. A significant improvement is visible in the 10–20 percent load range, up to more than 0.5 percent vs Competitor 3. This is mainly due to the reduced driving and switching losses, which are dominant in that load range. An improvement is also visible in the 60–100 percent load range, mostly related to lower typical  $R_{DS(on)}$  and switching losses, especially at turn-off.

The analysis of the operation with only one phase activated triggers some interesting considerations about a possible further improvement in the flatness of the efficiency curve.

Figure 45 shows in the same graph both the single phase (Conv1, up to 1500 W, red curve) and the dual-phase efficiency plot (up to 3000 W, blue curve).

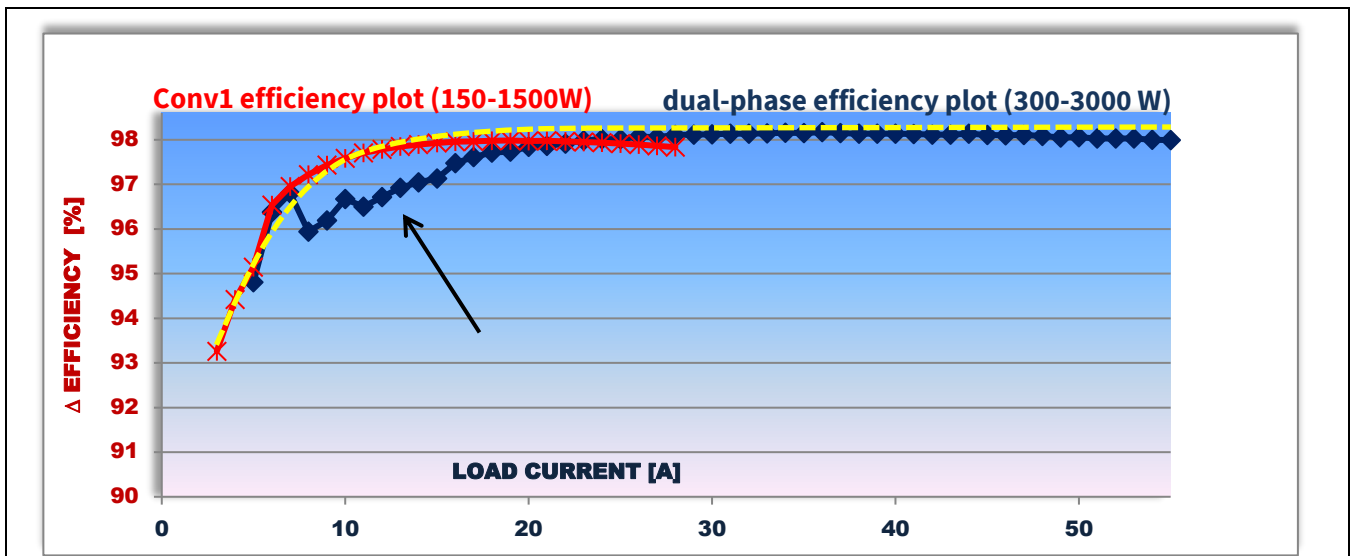


**Figure 49** Single versus dual-phase efficiency plot comparison

The operation of each of the two converters influences the phase shedding, specifically the output current level at which the Conv2 is activated/de-activated. Please refer to the definition of Conv1 and Conv2 as described in Section 4.2 of this document.

In fact the “valley” in the curve highlighted by the arrow in Figure 45 can be explained as follows: by reducing the output load from 100 percent to 10 percent load, at the total output current around 15 A, the SR MOSFET of Conv2 switches off, thus inducing the sudden reduction of efficiency in the visible valley. This is due to conduction on the SR MOSFET body diodes.

If the output current is reduced further, below the phase-shedding threshold, the Conv2 switches off and the Conv1 takes over, thus generating the natural sudden increase of efficiency seen in the plot.

We can therefore conclude that a possible way of achieving an even flatter efficiency plot is to switch off the Conv2 while its SR stage is still active. In that way we can minimize the valley described, and get a final curve like the dotted yellow line in Figure 45.

The phase shedding is confirmed to be a very important feature that really shapes the efficiency plot, according to the specific converter’s technical specification requirements.

#### Conclusion

## 6 Conclusion

The 3 kW dual-phase LLC demo board is the demonstration of how a mix of best-in-class CoolMOS™ and OptiMOS™ power device technologies with proper driver and control ICs enables a power converter design with superior performance and reliability features.

The demo board promotes a full Infineon solution suitable for a multi-phase/interleaving LLC design with phase shedding, by achieving a very high and flat efficiency plot, with the additional benefit of homogeneous heat spreading – necessary conditions to achieve high power density and increase reliability.

The concept enables reliable use of the HB LLC topology, which is the most cost-effective for high-efficiency designs. It demonstrates the good operation of the 600 V CoolMOS™ CFD7, a technology which enables all the benefits of a fast BD device in resonant applications without sacrificing any performance.

The OptiMOS™ 5 150 V series is also shown to have all the necessary features to guarantee efficient and reliable operation in the Synchronous Rectification stage of a complex dual-phase design.

In order to make the board test even more user friendly, a GUI has been designed, enabling engineers to easily interact with the converter during analysis on the bench.

The present document gives an overview of the most relevant design aspects and the considerations behind the decision to build such a demo board.

A bill of materials (BOM) and a detailed description of the most important active and passive components used, including the specification of the magnetic parts, are available inside this AN.

Details are also provided about the XMC4400-based digital control features, with an accurate description of the implemented algorithms.

Finally the performances are documented by captured waveforms and efficiency plots: all the results shown have been achieved with the 600 V CoolMOS™ CFD7 in the TO-247 package (IPW60R031CFD7), which results in the most suitable  $R_{DS(on)}$  for the analyzed output power range.

## 3 kW dual-phase LLC demo board

Using 600 V CoolMOS™ CDF7 and digital control by XMC4400

Technical Data Package (TDP)



### 7 Technical Data Package (TDP)

By clicking on the icon below, the reader can find a file providing a useful summary of all the technical and assembly features of the Infineon 3 kW dual-phase LLC demo board.

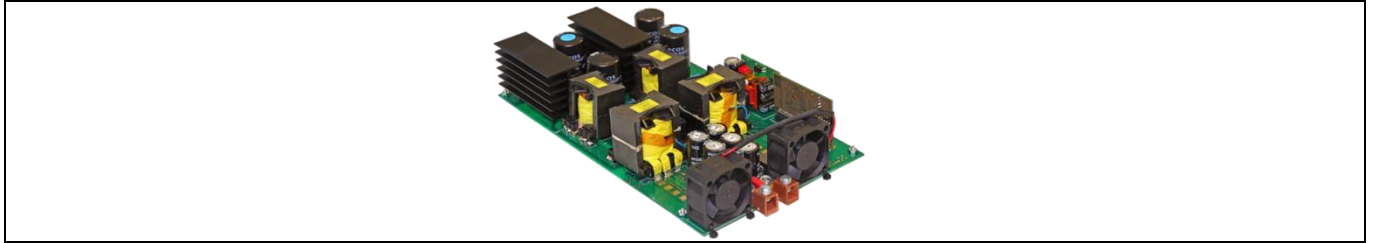


**Figure 50** Technical and assembly features of the Infineon 3 kW dual-phase LLC demo board.

The BOMs of the motherboard and the two daughter cards are available in this document. The CAD and Gerber files are available on request.

A procedure for functional testing is also included: this is exactly the same as that applied to each prototype during mass production.

## 8 Related resources

In the following links, you can find more detailed information about the devices used from Infineon and the magnetic components.

- [Primary HV MOSFETs CoolMOS™ IPW60R031CFD7](#)
- [Microcontroller XMC4400](#)
- [Advanced dual-channel gate drive 2EDN7524F](#)
- [Isolated gate drive 1EDI60N12AF](#)
- [Bias QR Flyback controller ICE2QR2280Z](#)
- [SR MOSFETs OptiMOS™ BSC093N15NS5](#)
- [Main transformer and resonant choke ferrite cores](#)

#### References

## 9 References

- [1] F. Di Domenico, J. Hancock, A. Steiner, J. Catly, P. Yelamos, A. Medina: “600 W Half-bridge LLC eval board with 600 V CoolMOS™ C7 and digital control by XMC™”, Infineon Technologies, May 2016. [Available online](#)
- [2] H. Figge, T. Grote, N. Froehleke, J. Boecker, P. Ide: “Paralleling of LLC resonant converter using frequency controlled current balancing”, in Proc. of IEEE Power Electronics Specialists Conference – PESC 2008, June 2008 pp. 1080–1085, IEEE APEC 2001, Volume 2, pp. 728–735
- [3] D. Medini, S. Ben-Yaakov: “A current-controlled variable-inductor for high frequency resonant power circuits”, in Proc. of IEEE Applied Power Electronics Conference – APEC, February 1994, pp. 219–225
- [4] E. Orietti, P. Mattavelli, G. Spiazzi, C. Adragna, G. Gattavari: “Two-Phase Interleaved LLC Resonant Converter With Current-Controlled Inductor”, 2009 Brazilian Power Electronics Conference
- [5] Zhiyuan Hu, Yajie Qiu, Yan-Fei Liu: “Digital Implementation of Load Sharing Method for Interleaved LLC Converters”, Department of Electrical and Computer Engineering, Queen’s University Kingston, ON, Canada, December 2013
- [6] Bong-Chul Kim, Ki-Bum Park, Gun-Woo Moon: “Analysis and Design of Two-Phase Interleaved LLC Resonant Converter Considering Load Sharing”, IEEE Energy Conversion Congress and Exposition (ECCE), 2009, pp. 1141–1144
- [7] Gang Yang “Design of a High Efficiency High Power Density DC-DC converter for Low Voltage Power Supply in Electric and Hybrid Vehicles”, Supélec, 2014
- [8] F. Di Domenico, A. Steiner, J. Catly, “Design of a 600 W HB LLC Converter using 600 V CoolMOS™ P6”, Infineon Technologies, August 2015. [Available online](#)
- [9] A. Steiner, F. Di Domenico, J. Catly, F. Stückler, “600 W Half-bridge LLC Evaluation Board with 600 V CoolMOS™ C7”, Infineon Technologies, June 2015. [Available online](#)
- [10] T. Fujihira: “Theory of Semiconductor Superjunction Devices”, Jpn. J. Appl. Phys., Vol. 36, pp. 6254–6262, 1997
- [11] Lawrence Lin, Gary Chang: “Primary-side MOSFET Selection for LLC topology”, Infineon Technologies, June 2014. [Available online](#)
- [12] F. Stückler, S. Abdel-Rahman, K. Siu: “600 V CoolMOS™ C7 Design Guide”, Infineon Technologies, May 2015. [Available online](#)
- [13] Dr. Arshad Mansoor, Brian Fortenbery, Peter May-Ostendop, et al.: “Generalized Test Protocol for Calculating the Energy Efficiency of Internal AC-DC and DC-DC Power Supplies”, Revision 6.7, March 2014
- [14] “XMC4400 Reference Manual”, April 2014. [Available online](#)
- [15] Matthias Kasper, Dominik Bortis, Johann W. Kolar: “Scaling and balancing of multi-cell converters”, 2014 International Power Electronics Conference (IPEC-Hiroshima 2014 – ECCE ASIA), 2014
- [16] Francesco Di Domenico, Alois Steiner: “Design of a 600 W HB LLC using 600 V CoolMOS™ P7”, Infineon Technologies, 2017
- [17] René Mente, “CoolMOS™ 600 V CFD7”, AN\_201708\_PL52\_024, Infineon Technologies, 2017

### Glossary

### Glossary

Abbreviation	Expanded form
ADC	Analog to Digital Converter
BD	Body Diode
CAD	Computer-Aided Design
CCU	Capture and Compare Unit
CLT	Coreless Transformer
CMTI	Common Mode Transient immunity
$C_{OSS}$	Output Capacitance $C_{OSS} = C_{DS} + C_{GD}$
$C_{o(tr)}$	Effective output capacitance, time related
COM	Communication port
$C_r$	Resonant capacitance
CSG	Comparator and Slope Generator
DAC	Digital to Analog Converter
DC	Direct Current
DMA	Direct Memory Access
DSP	Digital Signal Processor
di/dt	Steepness of current slope at turn-off/turn-on
EEPROM	Electrically Erasable Programmable Read-Only Memory
EMI	Electromagnetic Interference
$E_{OSS}$	Stored energy in output capacitance
ERU	Event Request Unit
FET	Field Effect Transistor
FPU	Floating Point Unit
$F_{sw}$	Switching frequency
GaN	Gallium nitride
GND	Electric ground
GUI	Graphical User Interface
HB	Half-Bridge
HS	High-Side
HRC	High Resolution Channel
HRPWM	High Resolution PWM
HV	High Voltage
IC	Integrated Circuit
ID	Drain-to-source current
IDE	Integrated Development Environment
$I_{out\_phase}$	Output current of one converter
$I_{res}$	Resonant current
LCD TV	Liquid Crystal Display television

# 3 kW dual-phase LLC demo board

## Using 600 V CoolMOS™ CDF7 and digital control by XMC4400



### Glossary

Abbreviation	Expanded form
$L_r$	Resonant inductance
$L_m$	Magnetizing inductance
LS	Low-Side
LV	Low Voltage
MAC	Multiplication and Accumulation unit
MOSFET	Metal Oxide Semiconductor Field Effect Transistor
NTC	Negative Temperature Coefficient thermistor
OCP	Over Current Protection
PFC	Power Factor Correction
PI	Proportional Integral controller
PSU	Power Supply Unit
PWM	Pulse Width Modulation
$Q_G$	Gate charge
$Q_{oss}$	Charge stored in the $C_{oss}$
QR	Quasi Resonant
RAM	Random Access Memory
$R_{DS(on)}$	Drain-source on-state resistance
$R_{g,on/off}$	Gate resistor applied at on and off transitions
SMPS	Switched Mode Power Supply
SPI	Serial Peripheral Interface
TDP	Technical Data Package
TTL	Transistor-Transistor Logic
UART	Universal Asynchronous Receiver-Transmitter
USIC	Universal Serial Interface Channel
ZVS	Zero Voltage Switching

### Revision history

### Revision history

Document revision	Date	Description of changes
V 1.0	2017-10-12	Initial release
V 1.1	2025-12-02	Life cycle review: Updated to the latest template

## Trademarks

All referenced product or service names and trademarks are the property of their respective owners.

**Edition 2025-12-02**

**Published by**

**Infineon Technologies AG**

**81726 Munich, Germany**

**© 2025 Infineon Technologies AG.**

**All Rights Reserved.**

**Do you have a question about this document?**

**Email: [erratum@infineon.com](mailto:erratum@infineon.com)**

**Document reference**

**AN201710**

### Important Notice

Products which may also include samples and may be comprised of hardware or software or both ("Product(s)") are sold or provided and delivered by Infineon Technologies AG and its affiliates ("Infineon") subject to the terms and conditions of the frame supply contract or other written agreement(s) executed by a customer and Infineon or, in the absence of the foregoing, the applicable Sales Conditions of Infineon. General terms and conditions of a customer or deviations from applicable Sales Conditions of Infineon shall only be binding for Infineon if and to the extent Infineon has given its express written consent.

For the avoidance of doubt, Infineon disclaims all warranties of non-infringement of third-party rights and implied warranties such as warranties of fitness for a specific use/purpose or merchantability.

Infineon shall not be responsible for any information with respect to samples, the application or customer's specific use of any Product or for any examples or typical values given in this document.

The data contained in this document is exclusively intended for technically qualified and skilled customer representatives. It is the responsibility of the customer to evaluate the suitability of the Product for the intended application and the customer's specific use and to verify all relevant technical data contained in this document in the intended application and the customer's specific use. The customer is responsible for properly designing, programming, and testing the functionality and safety of the intended application, as well as complying with any legal requirements related to its use.

Unless otherwise explicitly approved by Infineon, Products may not be used in any application where a failure of the Products or any consequences of the use thereof can reasonably be expected to result in personal injury. However, the foregoing shall not prevent the customer from using any Product in such fields of use that Infineon has explicitly designed and sold it for, provided that the overall responsibility for the application lies with the customer.

Infineon expressly reserves the right to use its content for commercial text and data mining (TDM) according to applicable laws, e.g. Section 44b of the German Copyright Act (UrhG).

If the Product includes security features:

Because no computing device can be absolutely secure, and despite security measures implemented in the Product, Infineon does not guarantee that the Product will be free from intrusion, data theft or loss, or other breaches ("Security Breaches"), and Infineon shall have no liability arising out of any Security Breaches.

If this document includes or references software:

The software is owned by Infineon under the intellectual property laws and treaties of the United States, Germany, and other countries worldwide. All rights reserved. Therefore, you may use the software only as provided in the software license agreement accompanying the software.

If no software license agreement applies, Infineon hereby grants you a personal, non-exclusive, non-transferable license (without the right to sublicense) under its intellectual property rights in the software (a) for software provided in source code form, to modify and reproduce the software solely for use with Infineon hardware products, only internally within your organization, and (b) to distribute the software in binary code form externally to end users, solely for use on Infineon hardware products. Any other use, reproduction, modification, translation, or compilation of the software is prohibited. For further information on the Product, technology, delivery terms and conditions, and prices, please contact your nearest Infineon office or visit <https://www.infineon.com>